Winter 12-2021

Structural Analysis and Vaccine Efficacy of Hla mutants

Kelly Tomaszewski

WASHINGTON UNIVERSITY IN ST. LOUIS
University College

Structural Analysis and Vaccine Efficacy of Hla mutants

by
Kelly L. Tomaszewski

A Thesis presented to
The Graduate School
of Washington University in
partial fulfillment of the
requirements for the degree
of Master of Arts in Biology

December 2021
St. Louis, Missouri

Table of Contents

List of Figures

Acknowledgments

First, I would like to acknowledge my mentor, Julie; without her I would not be where I am today. During undergrad, I received a Bachelor of Science in biology and started applying to physical therapy schools. When that didn't work out, I lost my direction. Though I've always been fascinated by biological sciences, I never imagined I could be a scientist, let alone do research at elite universities. I decided to apply to research positions anyway and ended up landing an interview with Julie at the University of Chicago. After the interview I called my mom and said, "I don't think I got the job. Plus, I did an awkward 'air handshake' as I was thanking Julie for her time." (face palm). To my surprise, I got a call back. I had hardly any prior lab experience and I remember Julie saying to me this will be "baptism by fire." She was right! There were often times I felt like I was treading water, doubting myself and my ability to work alongside the upcoming PhDs and MDs training in her lab. However, Julie was very patient as she helped me learn and develop the necessary skills to think like a scientist and become independent at the bench. Fast forward to nearly 10 years later, Julie has continued to guide and have faith in me. She has always been supportive in my professional and personal life and encouraged me to pursue a graduate degree. I couldn't be more grateful that Julie saw something in me I struggled to see in myself. It is a privilege to be able to do science under her supervision and continue to learn from her. I would also like to thank the "original" U of C members of her lab as well as the current members for a fun, supportive and inspiring atmosphere over the years.

Second, I would like to acknowledge my family. Moving away from family and friends to a new city was not easy, but they have made annual trips to visit me, and I never felt left out. I often come back to my phone with over 50 unread text messages from the "family group chat."

I especially want to thank my mom and dad for the frequent trips to St. Louis despite their busy schedules being the best grandparents to all my nieces and nephews.

Next, I would like to thank my best friend, Jenny. Having gone through graduate school herself and being alone in a new city, she knew just what to say to help me push through. We would often FaceTime to make dinner together and plan short trips to recharge. We have known each other for 25 years so she feels like family, and I am super thankful for our friendship and her support especially during this time.

Lastly, I would like to acknowledge my boyfriend, Matt. Though we have only been in each other's lives for a couple of years, he continues to be a very positive influence. In addition to being dependable, he gives me constant support and more balance in my life. After stressful days in lab, he helps my mind relax; he's always willing to help me with random DIY projects and has been a wonderful partner to explore Missouri with. He has also proven to be the best "dog dad" I could ask for, which has been a major help during this time. His support allowed me to focus and not feel guilty leaving my dog at home when experiments run long.

Kelly L. Tomaszewski

Washington University, December 2021

CHAPTER 1

INTRODUCTION

1.1 STAPHYLOCOCCUS AUREUS

Staphylococcus aureus (*S. aureus*) is a gram-positive bacterium that is both a common commensal on human skin, colonizing approximately 30-50% of healthy adults, as well as a major human pathogen [1,2]. The bacterium was first discovered in pus from surgical abscesses in the 1880s by Dr. Alexander Ogston. He noted a spherical shaped microorganism frequently present in the pus in abundant clusters resembling "bunches of grapes", to which he gave the name: *staphylococcus* (a Greek term translating to bunches of grapes)[3]. From this observation, he hypothesized that the staphylococci may be responsible for tissue inflammation and suppuration. Applying Koch's postulates, he injected pus containing the staphylococci into animals and observed the same abscess formation in these animals as he had observed in the surgical wound sites. He also found that no abscesses formed when injecting animals with pus where staphylococci were absent, further confirming his hypothesis. A few years later, a German physician, Friedrich Rosenbach, differentiated this strain from other staphylococci strains by the golden hue of the colonies, giving its final name, *Staphylococcus aureus* (aureus from the Latin term, gold) which roughly translates to "golden grapes" [4]. In addition to the gold pigmentation, other differentiating elements include coagulase positivity and mannitol fermentation [2].

Despite the important implications in skin infection and bacteremia originally described by Dr. Ogston, the pathophysiology of *S. aureus* remained poorly understood and understudied for the next couple decades. Staphylococcal research began to gain more traction with about one publication per year by the beginning of the 20th century, however, between 2010-2020, an average of 2,000 articles per year were published, making staphylococcus currently the most researched bacterium [4]. Penicillin was introduced in the 1960s that initially worked well in controlling infection however quickly became an evolutionary highlight for the bug. Though

initially successful in combating infections, treating patients became increasingly difficult as *S. aureus* strains gained resistance to antimicrobial treatments such as methicillin [4,5,6]. Methicillin resistant *S. aureus* strains (MRSA) were at first mostly a hospital acquired infection – affecting elderly patients, patients with comorbidities or patients infected through foreign-body and medical devices [1,5]. However, by the mid-1990s there was a sharp rise in the general population contracting MRSA infections, creating a public health crisis in U.S. emergency departments and other clinical settings. The community-acquired MRSA strains (CA-MRSA), such as USA300, were found to be genetically distinct and more virulent as compared to the hospital-acquired MRSA strains, with the ability to cause a wide range of infections in otherwise healthy people [5]. Though minor skin and soft tissue infections are most common, CA-MRSA is also a leading cause of severe and life-threatening sepsis, necrotizing fasciitis and bacterial pneumonia. In the early 2000s over 11 million people were infected with drug-resistant *S. aureus* each year, causing more than 500,000 hospitalizations and more than 20,000 deaths per year from severe infection. These incidents generated a massive economic burden, with an estimated annual cost between $8.7 billion to $14.5 billion from 1998 to 2003 [7]. Although this rate has declined over the past decade, mortality from severe infections remain at 20% and the CDC identified MRSA as one of the top 18 pathogens requiring immediate attention, listing it as a "serious threat" in the *Antibiotic Resistance Threats in the United States, 2019* report [8,9].

Two major hurdles for controlling *S. aureus* infections are the need for novel therapies and innovative vaccine design. Currently, vancomycin and daptomycin are the most effective FDA approved antibiotics to combat MRSA, however, rare cases of strains with reduced susceptibility and low-level resistance to these drugs have been observed in some clinical isolates[5]. Due to its proven ability to gain multidrug resistance, it is imperative to develop non-

antibiotic therapeutics to reduce mortality and morbidity [1,5]. While the clinical consequences of other pathogens have been mitigated through successful vaccination strategies, *S. aureus* poses many unique challenges. Over the past decade, vaccines designed to prevent invasive *S. aureus* infection have failed in human clinical trials, despite a variety of approaches [5,10].

Both the commensal and opportunistic nature of this bacterium have contributed to its success as a human pathogen. In contrast to other human pathogens where colonization is transient, *S. aureus* has evolved to coexist with humans in order to maintain persistent colonization. Remarkably, approximately 20% of the healthy human population is persistently colonized with *S. aureus* on the epidermal layers of skin, while 80% are intermittently colonized[11]. "Infections are initiated when a breach of the skin or mucosal barrier allows staphylococci access to adjoining tissues or the bloodstream. Whether an infection is contained or spreads depends on a complex interplay between *S. aureus* virulence determinants and host defense mechanisms" [2]. A major advantage for this pathogen is the arsenal of virulence factors with the ability to disarm both innate and adaptative immune responses resulting in a broader range of infections.

Types of virulence factors *S. aureus* utilizes are membrane damaging toxins, enzymes, cell-wall anchored proteins and anti-immune system factors to target antibodies and complement factors. Together these virulence factors can disarm both the innate and adaptive immune responses [2,10]. For example, Panton Valentine Leukocidin (PVL), Chemotaxis Inhibitor Protein of *S. aureus* (CHIPS) and Staphylococcal Complement Inhibitor (SCIN) all disrupt innate immunity defenses. PVL is a pore-forming cytotoxin that can lyse neutrophils through the binding of complement receptors C5aR and C5L2 on the surface of neutrophils. CHIPS and SCIN both inhibit different aspects of the complement cascade, dampening neutrophil activation,

recruitment and opsonin-induced neutrophil killing [13,14,15]. The cell-wall anchored protein, Staphylococcal Protein A (SpA) is a multifunctional protein and one of three *S. aureus* proteins that interfere with immunoglobulin function. SpA promotes escape from neutrophil phagocytosis by binding the F_c portion of host immunoglobulins IgG. This binding interaction positions the immunoglobulins in an abnormal orientation, creating a protective coating over the bacteria and rendering them unrecognizable to neutrophils. An alternative binding site on SpA can also act as a B cell superantigen to dampen adaptive immune responses. SpA binding to the F_{ab} region of IgM B cell receptors activates clonal expansion, triggering production of plasma B cells to almost exclusively recognize protein A, thus acting as a decoy antigen and biasing the immune response away from other *S. aureus* virulence factors. In addition, the alternative SpA binding site also binds to other V_H3^+ B cell receptors and initiates activation-induced apoptosis of B cells, reducing antibody production and the ability to mount an effective adaptive immune response[5,13,15,16]. Furthermore, it is speculated that superantigens such as enterotoxin B, also subverts adaptive immunity by inducing T-cell tolerance and receptor anergy [17].

In addition to PVL, *S. aureus* also secretes an array of diverse cytolytic toxins such as the bi-component leukocidins, hemolysins and phenol-soluble modulins (PSMs) that can lyse and disrupt cell membrane integrity. Toxin sensitive cell types include immune cells, epithelial and endothelial cells, platelets and erythrocytes [16,17,18]. Of the *S. aureus* virulence factors, alpha-hemolysin also known as alpha-toxin (α-toxin) or Hla, is one of the most prominent and best characterized due to its critical role in *S. aureus* disease pathogenesis [19].

1.2 Staphylococcus aureus: alpha-toxin

Historic Studies

The role of the α-toxin in human disease was highly debated for a few decades, however, nearly a century worth of studies has identified it as one of the most significant virulence factors *S. aureus* encodes [19,20]. Shortly after the initial discovery of *S. aureus*, culture supernatants from *S. aureus* isolates were observed to have toxic properties in animal models. Injections with the supernatants were significantly injurious causing inflammation, dermonecrosis and lethality in rabbit and guinea pig models [18,19,21]. It was not until decades later that rigorous investigation into *S. aureus* secreted proteins ensued, driven by a diphtheria vaccine incident in Bundaberg, Australia in 1928 resulting in twenty-one ill children with ultimately twelve deaths. The onset of illness was rapid and severe, within hours, 16 children suffered symptoms ranging from vomiting to fever and convulsions, and within two days, 12 of the children had died. Furthermore, all of the surviving children had abscesses at the site of immunization. Appointed by the Commonwealth of Australia, F. McFarlane Burnet sought out to find the causative agent of this tragedy. Burnet's investigation revealed that the diphtheria vaccine preparation was contaminated with *S. aureus* and concluded that substantial amounts of a toxic substance must have been secreted from the bacterium. Burnet further observed that the vaccine-contaminating strain as well as other *S. aureus* isolates all had the same multi-biological effects: hemolysis, dermonecrosis upon intradermal injection and acute death when injected intravenously into rabbits [18,19,21]. Burnet and colleagues also demonstrated successful active and passive immunization in naïve rabbits using formalin-treated *S. aureus* supernatants and serum collected from immune rabbits, respectively. Active or passive immunity protected the naïve rabbits from

lethal disease and also neutralized the hemolytic and necrotic activity of the *S. aureus* supernatants.

Continuing studies in the 1940s eventually led to the identification of two distinct secreted toxins, termed α and β toxin. Both α and β toxins had hemolytic capabilities leading researchers to speculate that both toxins and potentially other secreted toxins may be responsible for the toxicity from *S. aureus* supernatants [20,22]. Toxin profiling studies by Glenny and Stevens highlighted the differences between α and β toxins, demonstrating that the α-toxin had hemolytic, necrotic and acute lethal properties among several species, phenocopying the *S. aureus* supernatants. Another unique observation about α-toxin was the variation in hemolytic susceptibility among species. For example, human erythrocytes were observed to be much less sensitive to hemolysis, requiring a 400-fold-higher concentration of α-toxin to cause lysis as compared to rabbit erythrocytes [19,20,21,22]. Furthermore, rabbits had the lowest LD_{50} compared to all other species tested at just 2 μg/kg of body weight, highlighting the unique sensitivity of rabbit erythrocytes to the α-toxin [19,21].

Despite these significant findings across animal species, due to the relative insensitivity of human erythrocytes, the importance of the α-toxin in human disease was highly debated for decades. However, a notable study published in 1964 by Siegal and Cohen demonstrated that platelet-rich human plasma treated with α-toxin induced morphological changes and aggregation of platelets with subsequent procoagulant activity [19,21,23]. Since this discovery, multiple human cells have been shown to be susceptible to the toxin, including epithelial, endothelial and hematopoietic-lineage cells. Furthermore, the toxin was shown to induce diverse responses including spastic contraction in smooth muscle cells and liberation of lysosomal enzymes,

shedding light on how this toxin causes injury and defining significant features of cellular responses to intoxication [19,21].

Toxin classification

The notion that the α-toxin disrupts cell membranes through oligomerization and pore formation was derived from studies in the 1970s through the 1980s. Toxin-treated liposomes and nucleated cells treated with α-toxin leaked small molecules, corresponding to prior findings by Siegal and Cohen that the α-toxin formed finite lesions on membranes [21,23]. Furthermore, 10 nanometer ring-like structures with 6-7 subunits and a central pore of approximately 2-3 nanometers were visible by electron microscopy on cellular membranes when treated with high concentrations of the toxin. Other functional studies demonstrated that molecules leaked from toxin treated erythrocytes did not exceed 1-2 nanometers in diameter. These dimensions corresponded to the channel structure observed by electron microscopy that extended through the interior portion of the toxin oligomer [21,24]. Around the same time, the complement complex C5b-9 was also shown to form discrete lesions on cell membranes with visible ring-structures and was soon identified as the first pore-forming cytolysin. Knowledge from these experiments were applied to studies with the α-toxin where they were able to isolate the membrane-bound ring structures, determining that they formed stable amphiphilic oligomers. In addition, early studies using electron microscopy started to scratch the surface on the mechanism and function of the toxin by concluding the following: 1) α-toxin had a strong binding interaction with target membranes; 2) high concentrations formed 10 nanometer ring-like structures on cellular membranes as well as liposomal membranes devoid of protein, and 3) binding seemingly caused membrane damage and lysis [21].

In the 1980s a conceptual model of the α-toxin pore-formation was devised and hypothesized to be the primary mechanism of membrane damage. The model was as follows: the α-toxin is secreted as a hydrophilic molecule and upon binding to target membranes, oligomerizes to form a stable protein hexamer complex. The hexamer then undergoes a conformational change, enabling the structure to insert into the target membrane generating a hydrophilic channel across the lipid-bilayer forming a pore that disrupts membrane integrity [21,24]. Several studies thereafter confirmed this finding, and the α-toxin was the first identified pore-forming bacterial toxin. The α-toxin became the prototype of β-barrel pore-forming toxins as these studies helped identify several other proteinaceous toxins that damaged cell membranes in a similar manner [21].

Toxin structure, function and regulation

Encoded in the core-genome of *S. aureus* by a single copy of the 960-bp *hla* gene, the α-toxin is initially produced as a 319-residue precursor. The precursor includes a 26-residue α-helical signal peptide which is cleaved, and the α-toxin is then processed to yield a mature secreted protein of 293 amino acids weighing 33.2 kDa [18,19,25,26]. The toxin was initially thought to aggregate to form a hexamer, however, in 1996 Song et. al solved the crystal structure of the fully assembled pore, revealing the oligomer structure to be a heptamer, containing seven protomer subunits [18,19,27]. These studies tremendously advanced the knowledge and resolution of the toxin structure as well as the functional model of toxin assembly. The mature toxin is secreted as water-soluble monomers and upon binding to susceptible cells, seven monomeric subunits oligomerize to form a 10-nanometer stable pre-pore heptamer. By an unknown mechanism, each protomer from the pre-pore structure partially unfolds, creating a transmembrane β-barrel which forms a 2-3 nanometer lytic pore [18,19,27,28,29]. Interestingly,

circular dichroism spectrum studies revealed that the mature toxin, including the intramembranous domains that form the central pore, is predominantly composed of β-strands with little to no α-helical structure [19,30]. Furthermore, the crystallographic studies showed that the fully assembled toxin resembles a mushroom-shape, 100Å wide by 100Å in height with an inner pore diameter of 14Å [18,31]. These studies also defined the three structural domains: (1) the extracellular cap domain; (2) the C-terminal rim domain; and (3) the N-terminal stem domain. The cap domain contains seven β sandwiches and the amino latch sequence (Ala_1-Val_{20}) of each protomer, which make extensive interactions with the adjacent protomer, contributing to the stability of the complex. The cap protrudes from the lipid bilayer surface, exposed to the aqueous environment and shapes the entry of the pore. The rim domain has fewer protomer-protomer interactions than the other domains but has direct contact with the lipid bilayer and projects from the underside of the heptamer. The inner surface of the rim domain and the upper portion of the stem domain, known as the rim–stem crevice, contain residues important for phosphocholine binding to the cellular membrane. The stem domain forms the membrane-perforating β-barrel pore, to which each protomer contributes two β-strands from a glycine-rich sequence, Lys_{100}-Tyr_{148}, forming a continuous β-sheet. Once fully assembled, the hydrophobic residues are positioned towards the lipid membrane and hydrophilic residues towards the lumen of the channel [18,19,27,32].

Toxin expression is orchestrated by several global regulatory systems within the *S. aureus* genome. Two-component systems and cytoplasmic regulators act as an interconnected network to tightly regulate toxin expression, secretion as well as bacterial survival within the host environment [18,19,33]. The most important and best studied systems include the accessory gene regulator (*agr*), the staphylococcal accessory protein effector (*sae*), and the staphylococcal

accessory gene regulator (*sarA*). The *agr* operon primarily controls toxin expression through a peptide quorum-sensing system and the regulatory RNA molecule, RNAIII. During late log to stationary phase of *S. aureus* growth, an accumulation of the secreted autoinducer peptide (AIP) is sensed by the histidine kinase receptor, AgrC and activates the AgrC/AgrA two-component system. AIP binding to AgrC, phosphorylates the receptor which in turn activates the intracellular response regulator AgrA [19,33]. AgrA then binds to the P3 promotor of the *agr* locus, initiating the production of RNAIII, thus enabling toxin expression and secretion. Maximum toxin production is reached during the stationary growth phase and rapidly secreted into the environment, with only 1% remaining cell associated [19,33,34,35]. Though this system primarily regulates toxin expression, the two-component system, SaeR/S, and the cytoplasmic regulatory system, SarA, fine-tune toxin expression through modulation of *agr* activity and simultaneously coordinate responses to the changing host environment, ensuring optimal pathogen function and survival [33,36,37].

1.3 Role of alpha-toxin in S. aureus Disease

While *S. aureus* has many virulence factors to promote disease, strains that have intact and/or increased expression of α-toxin are hypervirulent compared to other strains. The first cases of severe CA-MRSA infections in the U.S. were caused by isolates from the USA400 background. However, in the early 2000s, USA400 essentially disappeared and was replaced by USA300 which was found to have increased virulence compared to USA400 and HA-MRSA strains in a rat pneumonia model [18,38]. Genome sequencing revealed that the major difference between USA300 and less virulent strains was the expression of core global regulatory elements *agr* and *sae*, which correlates to the amount of α-toxin produced [18,19,38]. DeLeo et al showed that

HA-MRSA isolates containing mutations in the *agr* locus, which resulted in a loss of α-toxin expression, are less virulent in murine models of pneumonia and bacteremic infection [18,39]. Furthermore, Montgomery et al demonstrated that strains harboring a deletion of either the *agr* or *sae* loci also results in complete loss of α-toxin expression with greatly reduced mortality in murine pneumonia as well as the complete absence of dermonecrosis in skin infection [18,40]. These studies highlighted the significance of the global regulators in *S. aureus* pathogenesis, however, PVL is another pore forming toxin important in pneumonia infection and also regulated by *agr* and *sae*. Bubeck Wardenburg and others demonstrated that the α-toxin rather than PVL is absolutely necessary for full virulence of *S. aureus* disease. Deletion of the *hla* locus eliminated the ability of USA300 to cause lung infection, while deletion of the *pvl* locus did not affect the overall mortality in *S. aureus* pneumonia. The same phenotype was also observed in several other infection models such as skin, bloodstream, and corneal infections [18,41,42,43]. Together, these studies conclude that the critical factor for *S. aureus* pathogenesis is the presence of the α-toxin. Experimental models and epidemiological data highlight the notion that increased α-toxin expression is an advantage for the epidemic USA300 strain and because of this has the ability to cause invasive infection in otherwise healthy individuals. In contrast, this genetic advantage is not essential to cause infection in hospitalized patients likely due to an immunocompromised state with underlying health conditions.

1.4 Discovery of the alpha-toxin receptor, ADAM10

Early studies theorized that the receptor for the α-toxin may be a lipid moiety stemming from the observation that the toxin can bind and lyse protein-free membranes with a specific composition of phospholipids [18,19,21,44,45]. At high concentrations, the α-toxin can bind and lyse

liposomes composed of phosphatidylcholine or a combination of sphingomyelin and cholesterol. Depletion of cholesterol or sphingomyelin on rabbit erythrocytes or susceptible cells abolishes high-affinity toxin binding [18,19,46,47]. Additional studies found that exogenous phosphatidylcholine antagonizes toxin binding and thus reduces toxin-mediated hemolysis of rabbit erythrocytes. Furthermore, phosphatidylcholine is also required for the function of other staphylococcal pore-forming exotoxins, such as gamma-hemolysin and bicomponent leukocidins [18,32,48]. X-ray crystallographic studies with the heptamer and phosphatidylcholine provided even more compelling evidence as it showed direct binding of the rim-stem crevice of the toxin and phosphatidylcholine head groups, glycerophosphocholine and di-propanoyl phosphatidylcholine. These studies also revealed two critical residues in the rim domain, W179 and R200, which have side chains that protrude into the crevice, creating an attractive binding pocket for the headgroups. These residues are also conserved in bicomponent leukocidins, suggesting a structural requirement for pore-forming toxin binding and functionality on cellular membranes[18,32].

Though these studies provided key observations about the lipids necessary for toxin binding and function, a proteinaceous receptor was still suspected due to the exquisite cell type specificity and species specificity exerted by the α-toxin. The earliest and most drastic example of differing susceptibility is between rabbit erythrocytes and human erythrocytes at low nanomolar amounts of toxin can lyse rabbit erythrocytes, whereas micromolar concentrations are required to lyse human erythrocytes [19,44]. Other major observations that suggested a proteinaceous receptor were: 1) treatment with pronase, a non-specific protease, reduces rabbit erythrocyte sensitivity to α-toxin; 2) surface binding studies using radioiodinated α-toxin estimated 1,200 – 5,000 binding sites per rabbit erythrocyte, making them 16,000 times more

susceptible to hemolysis compared to human erythrocytes; 3) low concentrations of toxin binding to rabbit erythrocytes was saturable, time and temperature dependent which are characteristics indicative of a specific ligand-receptor interaction; and 4) treatment with high concentrations of toxin on either rabbit or human erythrocytes was non-saturable and non-temperature dependent, indicating a non-specific nature of toxin binding [18,44,45,49]. Together these findings revealed two modes of toxin binding that supported the proteinaceous receptor hypothesis and explained the lipid binding: where at low concentrations, the toxin utilizes a proteinaceous receptor as a high affinity binding site and at high concentrations the toxin binds non-specifically to lipid moieties on cellular membranes to facilitate binding and lytic function. Moreover, these findings suggested that human erythrocytes may lack the high affinity binding receptors and began to explain why certain cell types and species are more or less resistant to toxin-mediated lysis due to varying expression of the proteinaceous receptor [44,45,49].

Initially, pore formation was thought to be the major source of α-toxin-induced injury to the host, however, the discovery of the α-toxin proteinaceous receptor, ADAM10, uncovered a dual mechanism which greatly advanced the knowledge of downstream pathologic effects of the toxin-receptor interaction. In 2010, Wilke and Bubeck Wardenburg took advantage of the species-specific receptor expression and purified the presumed α-toxin receptor using a biochemical approach. A ~65kDa protein was isolated from rabbit erythrocyte membranes using a non-toxigenic α-toxin mutant, GST-Hla_{H35L}, which is capable of binding but devoid of pore formation. This protein was unable to be recovered from human erythrocytes, consistent with prior data demonstrating the lack of binding sites and cytotoxicity with toxin treatment. Mass spectrometric analysis identified the isolated protein as ADAM10 (A Disintegrin and

Metalloprotease 10), a zinc-dependent metalloprotease that is surface expressed on essentially all cell types as a type I transmembrane protein.

1.5 Role of alpha-toxin and ADAM10 in S. aureus Disease

Further studies by Bubeck Wardenburg provided concrete evidence that ADAM10 was likely the α-toxin receptor due to the downstream cellular effects of the Hla–ADAM10 interaction and its important role in *S. aureus* disease pathogenesis. First, they showed ADAM10 facilitates α-toxin binding to eukaryotic cells and ADAM10 expression is required for cytotoxicity. This was demonstrated using a panel of human epithelial cell lines with varying levels of ADAM10 expression showing a linear correlation between ADAM10 expression and toxin binding. In addition, siRNA-mediated knockout of ADAM10 reduced toxin binding and cytotoxicity. Second, α-toxin binding induced ADAM10 relocalization to caveolin-1-enriched lipid rafts and subsequent barrier disruption via altered focal adhesion signaling. Caveolin-1 has been previously shown to be important for toxin oligomerization, however, this data demonstrated that the toxin requires both ADAM10 and membrane binding within caveolin-1-enriched rafts. This toxin-receptor complex then utilizes the caveolin-1 platform to initiate the clustering of signaling molecules and pore formation leading to the perturbation of cellular barriers [18,45]. As ADAM10 plays a role in multiple cellular homeostatic processes, tissue development and immunologic function, these findings shed light on the hypothesis that the α-toxin may alter normal ADAM10 activity [45,50,51]. In addition, since α-toxin mediated injury is dependent on the presence of ADAM10, this led to the hypothesis that animal models lacking ADAM10 should be protected from the effects of the toxin in *S. aureus* disease.

Over the last decade, Bubeck Wardenburg and colleagues developed several animal models highlighting the role of ADAM10 in *S. aureus* disease pathogenesis and revealed an unexpected mechanistic insight of α-toxin induced injury. Since ADAM10 is involved in various developmental processes and tissue homeostasis, a global knockout of the *Adam10* gene in mice is embryonic lethal at E9.5 [18,50,52]. To circumvent this, *in vivo* studies utilized conditional or inducible *Adam10* knockout (*Adam10*$^{-/-}$) mouse lines in various tissues such as epithelial (alveolar and epidermal keratinocytes), endothelial, platelet and immune cells (myeloid lineage and T cell). Bubeck Wardenburg showed mice harboring a conditional *Adam10*$^{-/-}$ in alveolar epithelium or endothelial cells are largely protected from lethal pneumonia or bloodstream infection compared to control mice [52,] and Alfano, et al unpublished data. Similarly, epidermal keratinocyte *Adam10*$^{-/-}$ mice challenged with subcutaneous infection resulted in smaller abscesses as well as the absence of tissue dermonecrosis; a hallmark of α-toxin injury [42,52]. Interestingly, *Adam10*$^{-/-}$ on myeloid lineage or platelet cells revealed immunomodulatory effects of the Hla-ADAM10 complex. Subcutaneous infection on myeloid lineage *Adam10*$^{-/-}$ mice resulted in exacerbated skin lesions yet afforded protection against lethal pneumonia infection [53]. Furthermore, the loss of *Adam10* on either platelet or myeloid lineage cells succumb to bloodstream infection. However, *Adam10* double-knockout mice harboring a myeloid lineage *Adam10*$^{-/-}$ with either epithelial or platelet *Adam10*$^{-/-}$ are highly protected against *S. aureus* infection [54].

Further investigation into the molecular mechanisms of the toxin-receptor interaction uncovered a unique characteristic of the α-toxin. At sub-lytic concentrations, the toxin pore causes rapid upregulation of ADAM10 metalloprotease activity resulting in the pathologic cleavage of native ADAM10 substrates [52]. For example, in skin, lung and bloodstream infection,

barrier disruption and subsequent disease progression is associated with the pathologic cleavage of adherens junctional proteins, E-cadherin and VE-cadherin induced by α-toxin. Furthermore, these animal models uncovered the systemic effects of immunomodulation and altered cytokine and chemokine signaling induced by the α-toxin. While myeloid cells such as neutrophils and macrophages are more resistant to the lytic action of the α-toxin due to the intrinsic low level of surface expression of ADAM10, exposure to α-toxin dampens their ability to produce IL-1ß. This dampened response intensifies the epidermal tissue damage seen in myeloid lineage *Adam10*$^{-/-}$ mice in skin infection yet provides protection against pneumonia infection since a proinflammatory state contributes to lung injury [53]. Another important insight from the platelet and myeloid *Adam10*$^{-/-}$ mice showed that the Hla-ADAM10 interaction effects the immune response by altering platelet activation and promotes neutrophil inflammatory signaling. Moreover, α-toxin not only damages platelets which prevents endothelial barrier repair, but also facilitates formation of injurious platelet-neutrophil aggregates, contributing to lung and liver injury. Further supporting the direct role of ADAM10 in *S. aureus* infection, an ADAM10 specific inhibitor blocks cadherin proteolysis, preserving the tissue barriers and significantly attenuating pneumonia and sepsis lethality and dermonecrosis in skin abscesses [41,42,52].

These studies provided several valuable insights not only for *S. aureus* pathogenesis but also for pore-forming toxin biology in general as this was the first time a β-barrel pore-forming toxin was shown to interact with a receptor in this way. Moreover, these studies explained the remarkable ability of a single bacterial toxin to coordinate progressive disease through tissue specificity and modulation of host immunity.

Chapter 2

alpha-toxin and ADAM10 Binding Interaction

2.2 Important Residues in Toxin Binding and Oligomerization

Structure-function analysis of α-toxin through scanning mutagenesis has revealed key residues for toxin binding and function. Residues R_{66}, E_{70}, W_{179}, R_{200}, D_{254} and D_{276} located in the rim and β-sandwich and are required for toxin membrane binding. Cysteine mutants of these residues maintain full toxin assembly; however, the lytic function is greatly reduced due to the cellular binding defect [32,57]. Furthermore, mutations at residues D_{24}, K_{110} and D_{152} retain membrane binding but impact pore-formation as they are arrested in the oligomer pre-pore, thus disabling the lytic function of the toxin pore. Interestingly, the N-terminal segment known as the amino latch undergoes a conformational shift, latching onto the neighboring protomer which stabilizes the toxin oligomer [55,57]. Within the N-terminal segment, H_{35} is a critical residue located at the interface between protomers and aids in the stabilization and pre-pore to pore transition. During toxin assembly, H_{35} moves into a hydrophobic environment initiating the insertion of the stem domain into the membrane. Mutations at this position retain membrane binding yet renders a completely inactive toxin as the interprotomer connections are destabilized and therefore unable to fully assemble into the pore [55,56,57,58].

Examining the pore-forming mechanism in more detail remained a challenge for years as only the fully assembled toxin crystal structure was available. However, in 2015 Sugawara et. al generated crystal structures using a double mutant ($W_{179}A/R_{200}A$) and a single mutant ($H_{35}A$) that allowed the toxin to be visualized in the soluble monomeric and pre-pore structures, respectively [58]. Structure comparison of the monomeric, pre-pore and fully assembled crystal structures uncovered a dynamic pore-formation mechanism. First, the pre-stem in monomeric form is secured to the cap domain by a key hydrogen bond between residues D_{45} and Y_{118}. Next,

as the pore assembles, hydrophobic interactions between the cap domain and the N-terminal amino latch of the adjacent protomers play a key role. The N-terminal amino latch folds into a short helix, creating a hydrophobic core with residues of the adjacent protomer, stabilizing the extended amino latch within the pore state. Simultaneously, this conformational shift destroys the key hydrogen bond between D_{45} and Y_{118}, allowing the pre-stem to be released and fold down into the pore. Lastly, the release of the pre-stem exposes the hydrophobic surface on the cap domain which binds the amino latch of the adjacent protomer, further stabilizing the pore. Of note, two hydrophobic residues I_5 and I_7 important in the structure of the amino latch, also aid in the conversion of the amino latch from monomer to oligomer. These analyses also showed that the toxin pore is formed in a two-step process where the extracellular β-barrel is formed in the pre-pore state, and the transmembrane region inserts into the membrane to form the pore, which completes the pore formation. This mechanism is consistent with other two-component staphylococcal pore-forming toxins [58].

2.2 ADAM10 structure and domains

ADAM10 belongs to the ADAM family of zinc-dependent metalloproteases found in all vertebrate tissues and involved in several processes from fertilization and neurogenesis to wound healing and inflammation [51]. These proteins have many important regulatory functions and act as an ectodomain sheddase, releasing a variety of cell-surface proteins such as growth factors, cytokines, cell adhesion molecules and receptors as well as cleave and remodel extracellular matrix components. Additionally, the release of the soluble portions of the ectodomains can influence intracellular cell signaling pathways. Due to the overall critical role of ADAMs, dysfunction of these proteins is implicated in a wide range of diseases including rheumatoid

arthritis, Crohn's disease, diabetes, Alzheimer's, cardiac hypertrophy, cancer and microbial infections [51,59,60,61].

Zinc metalloproteases are divided into subgroups based on the primary structure of their catalytic site and further divided by the domains they contain [62]. A distinguishing feature of the ADAM subgroup is the presence of a disintegrin domain and a conserved methionine β-loop structure near the zinc-binding motif, a key characteristic of the metzincin superfamily of zinc metalloproteases [62,63,64]. ADAMs are single membrane spanning proteins that share a common modular structure. ADAM10 and its closest homologue, ADAM17, have a transmembrane domain that connects to a C-terminal cytoplasmic tail and three ectodomains containing an N-terminal signal sequence preceding a prodomain, followed by a metalloprotease, a disintegrin and a cysteine-rich domain [51,61]. Furthermore, these proteins are synthesized as zymogens, where the immature form of the protein contains an N-terminal prodomain that gets removed during processing, converting the inactive precursor into a mature active protease upon surface expression [64].

ADAM10 domain function

The N-terminal signal sequence directs ADAMs to the secretory pathway and the prodomain keeps the metalloprotease domain inactive through a conserved cysteine residue that acts as a cysteine switch. This switch within the prodomain sequesters the required active site zinc ion, ultimately preventing the metalloprotease activity. The prodomain also acts as a chaperone, aiding in the proper folding and maturation of ADAMs. The metalloprotease domain engenders the ectodomain sheddase function through zinc and water ions necessary for the hydrolytic processing of protein substrates. The active site consensus sequence contains three

conserved histidine residues (HExxHxxGxxH) and a downstream methionine that lies within the 'met turn motif' that faces the active site. The disintegrin domain is a distinguishing feature of the ADAM proteins and mediates cell-cell adhesion [60,62,65]. Furthermore, this domain interacts with integrins and was first discovered in snake venom as they disrupted specific platelet integrins and inhibit platelet aggregation. The cysteine-rich domain works together with the disintegrin domain to facilitate extracellular protein interactions and are both involved in the regulation of catalytic activity, substrate targeting and recognition and removal of the prodomain[60,65,66,67]. Furthermore, the surface exposed residues in these domains are highly divergent among the ADAMs which is consistent with the various substrate profiles of the ADAM family members [60,66]. The transmembrane domain passes through the lipid bilayer one time and connects the ectodomains to the C-terminal cytoplasmic tail. The cytoplasmic tail has been suggested to aid in several signaling events including the inside-out regulation of the metalloprotease activity, the outside-in regulation of cellular signaling, and the control of maturation and subcellular localization. Furthermore, this domain also has potential phosphorylation sites for serine-threonine and/or tyrosine kinases that may influence maturation, activity and intracellular transport [60,62].

2.3 Hla-ADAM10 Binding and The Role of ADAM10 Activity in Disease

While ADAM10 metalloprotease activity has been shown to be upregulated in several *S. aureus* disease models, it was unclear if toxin pore-formation and ADAM10 activation were both required to mediate disease pathogenesis. Furthermore, the toxin-receptor interaction interface remained elusive as the toxin does not bind to purified ADAM10, likely due to the requirement of the receptor to be in a specific conformation as it is within the cellular membrane. Recent structure-function analysis data of the Hla-ADAM10 complex from the Bubeck Wardenburg lab

revealed that the metalloprotease domain is necessary for Hla binding and cytotoxicity. Moreover, a limited stretch of residues conserved across species in ADAM10 mediate this interaction, providing molecular insight on toxin specificity of receptor utilization. Interestingly, *in vitro* and *in vivo* analysis of a catalytically inactive ADAM10 mutant harboring a point mutation in the active site ($ADAM10_{E384A}$) revealed that ADAM10 enzymatic activity is not required for Hla binding but remains essential for cytopathic effects on lung epithelial cells *in vitro*, as well as pathogenesis in a lethal mouse model of *S. aureus* pneumonia and sepsis. While transgenic mice expressing wild-type bovine ADAM10 succumbed to infection, mice expressing the catalytically inactive bovine $ADAM10_{E384A}$ were equally recalcitrant to *S. aureus* pneumonia and sepsis as ADAM10 knock-out mice, illustrating the exquisite biological coupling of toxin pore formation and ADAM10 metalloprotease activity in pathogenesis (Tomaszewski and Berube unpublished data, Alfano unpublished data).

Due to the complexity and instability of ADAM10 as a transmembrane protein, the crystal structure of this protein is only partially solved, leaving structural and mechanistic questions open and only predicted. However, recent studies by Seegar et al. determined the ectodomain crystal structure which provided valuable insight into the regulation of ADAM10 activity, which may be important for toxin binding and function. They proposed a model of ADAM10 activation where ADAM10 switches between an ‘open’ and ‘closed’ confirmation for substrate accessibility [61]. In the closed confirmation, the cysteine-rich domain partially occludes the active site on the metalloprotease domain rendering ADAM10 inactive. In addition, they identified an ADAM10 antibody, which, upon binding, alters the shape of the ADAM10 protein, causing the displacement of the cysteine-rich domain from the active site and upregulation of ADAM10 metalloprotease activity.

These findings along with the binding and catalytic activity data led us to two key hypotheses: 1) The activity state and structural conformation of ADAM10 may differentially influence Hla binding and function and 2) the tertiary structure of Hla and how that effects the interaction with ADAM10 may be an important implication in the immune response and disease outcome. In the closed confirmation, the cysteine-rich domain partially occludes the active site on the metalloprotease domain which may impede toxin binding. Furthermore, previous studies using a small molecule inhibitor of the active site precludes Hla-ADAM binding [41], further supporting this idea. Identifying the exact mechanism and structural interface between the toxin and receptor could provide greater insight into the biologic function of pore-forming toxins in general. In addition, whether the toxin can interact with ADAM10 or not, may influence different immune pathways that shape the disease outcome and subsequent immunity.

Chapter 3

Structural analysis and vaccine efficacy of Hla mutants

3.1 Introduction

Past vaccine clinical trials

While anti-bacterial vaccines have significantly mitigated other diseases such as *B. pertussis, C. diphtheriae*, *C. tetani*, and *S. pneumoniae*, generating a successful *S. aureus* vaccine has remained a major challenge in the field. In the last two decades, a substantial amount of effort has been focused on *S. aureus* vaccine development generating 16 candidate preparations; however, none were proven to be successful in clinical trials [68,69,70]. In fact, 10 out of the 16 candidate immunization strategies failed human clinical trials, including three high-profile Phase 3 active vaccine candidates. Furthermore, the remaining vaccine candidates are either at a stand-still with no further development after trial completion or studies are ongoing without any reports on the data outcome [10,12,69]. Nonetheless, these failed efforts have provided researchers with insight into the immunization design flaws and unique challenges of *S. aureus*.

The fact that *S. aureus* is a commensal of the skin and has evolved with humans allows this pathogen to remain as a persistent or intermittent colonizer, creating a baseline 'host tolerance' which is uncommon compared to other pathogens. Furthermore, most adult humans have high antibody titers against several staphylococcal antigens, however, these antibodies do not provide significant protection against *S. aureus* infection [70]. Recent studies by the Bubeck Wardenburg lab showed that *S. aureus* skin infection causes a defect in adaptative immunity, specifically the T cell response and loss of dendritic cells due to the α-toxin (Hla). In addition, Hla exposure caused more than a 2-fold reduction in the number of antigen-specific $CD4^+$ T cells that respond to *S. aureus* infection, while toxin neutralization through active or passive immunity restores T cell development [71]. These studies led to the hypothesis that early exposure to *S.*

aureus and α-toxin causes an 'original antigenic sin' phenomenon in which subsequent exposures only amplifies the initial non-protective immune response, leaving the host susceptible to disease. This phenomenon has been described in other pathogens such as influenza, SARS-CoV-2, dengue fever and HIV where reinfection is common and/or the immune response is defective due to a dominant antigen from initial infection perpetuating the flawed immune response to succeeding infections [72-76].

3.2 Vaccine Candidate Design and Hla-ADAM10 Mouse Model

Since most of the population is exposed to the α-toxin early in life - either through commensal colonization or *S. aureus* infection; one potential explanation for the clinical trial failures is that all immunization strategies have been tested in adults. In fact, these adults all harbored evidence of pre-exposure to the α-toxin where their immune system has already been primed and programmed with a potentially unfavorable immune response. In addition, multiple *S. aureus* virulence factors have been tested, however, Hla is perhaps one of the most influential virulence factors *S. aureus* encompasses and has been previously demonstrated to be an effective immunogen early upon its discovery [21]. Solely targeting Hla through passive and active immunization has also been proven to be effective against *S. aureus* disease in multiple pre-clinical studies from Bubeck Wardenburg and others [77-82].

Due to the tremendous amount of evidence on the deleterious effects of the α-toxin in *S. aureus* disease and the role of the Hla-ADAM10 complex that we have previously described; we propose a two-fold strategy for a novel *S. aureus* vaccination design: Strategy 1) neonate vaccination aimed to neutralize Hla will improve the adaptative immune response by allowing a more diverse T-cell repertoire to be generated and therefore provide long-lasting and effective

protection against subsequent insults later in life; Strategy 2) the Hla and ADAM interaction is important to consider in the design of vaccine candidates as Hla mutants that disrupt or preserve this interaction may be key in mounting a more effective immune response.

We sought to test the hypotheses from Strategy 2 by immunizing mice with Hla mutants that would alter or preserve the binding efficiency to ADAM10 as well as change the tertiary structure of the toxin. The three candidate vaccinations include a single substitution mutant H35L, and two double mutants D45A/Y118F and R66C/E70C. Residue H35 is located at the protomer-protomer interface of each monomer within the cap domain and is critical for the stabilization of the oligomeric structure. Substitution of the histidine residue to leucine destabilizes the oligomeric structure, thus abolishing toxin activity and is not predicted to alter the structure of the monomer. Furthermore, this mutation has also been shown to maintain binding to ADAM10 comparable to wild-type toxin [45,52]. A key hydrogen bond between residues D45 located in the cap domain and Y118 located in the glycine-rich loop keep the pre-stem intact with the cap domain before the pre-pore to pore transition. Substitutions at these residues is predicted to disengage the pre-stem from the cap domain and considerably alter the monomeric and tertiary structure as well as expose the amino latch. Residues R66 and E70 reside in the rim domain and have been previously demonstrated to be important for membrane binding. Substitution of these residues should alter the toxin binding properties, therefore diminishing the Hla-ADAM10 interaction but maintain a normal toxin structure.

In addition to these studies, we generated a mouse model as a tool to visualize the Hla-ADAM10 interaction. Visualizing the binding interface as well as the conformation of these

proteins will allow us to gain structural insight into the complex molecular actions that conclude with toxin pore formation and ADAM10 activation.

3.2.1

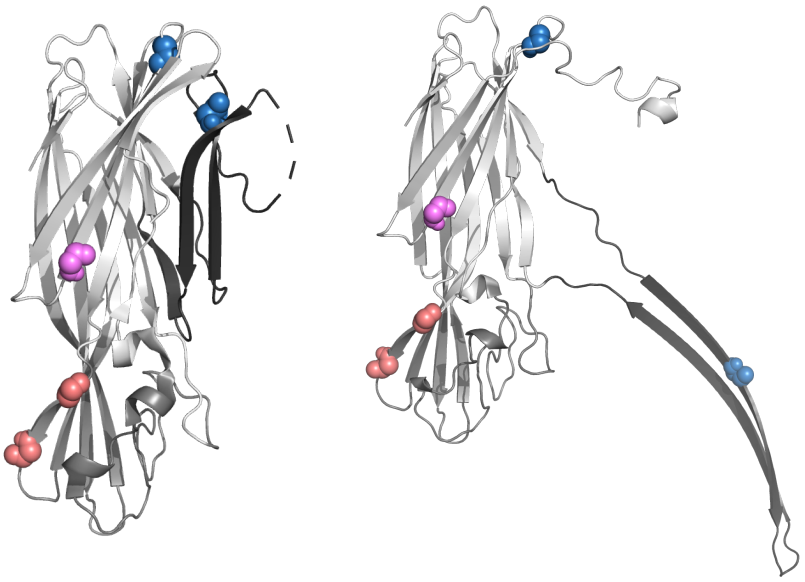

Figure 3.2.1 Hla mutant schematic

Crystal structures of monomeric alpha-toxin (left) and fully assembled heptameric alpha toxin (right). Residue H35 is colored lavender and located in the mid cap domain (light gray), residues D45 and Y118 are colored blue located in the upper cap and stem domains (light gray and dark gray) respectively, and residues R66 and E70 are colored orange and located in the rim domain (medium gray).

3.3 Results

3.3.1 Characterization of mutant Hla variants: rRBC Lysis

To assess the effect of mutations on the activity of the toxin, rabbit RBCs were incubated with a range of purified toxins (Supp. Fig. 3.7.1) and the capacity to lyse rabbit RBCs following incubation was determined. Absorbance of lysate at 450nm was measured and used to determine percent lysis (Fig. 3.3.1A) Mutant H35L is completely inactive at all concentrations, as expected from prior literature, while D45A/Y118F and R66C/E70C maintained some ability to lyse cells at high concentrations. At 10 μg/mL, D45A/Y118F has no detectable lysis, however, concentrations above this restores lytic ability though significantly reduced compared to wild type or R66C/E70C (data not shown). R66C/E70C is significantly more active than D45A/Y118F as rabbit RBCs treated with this mutant results in over 80% lysis at 10 μg/mL. However, R66C/E70C is less active than wild type as it loses the ability to lyse as the toxin is diluted but still results in over 50% lysis at the second dilution of toxin (5 μg/mL). Toxin activity is not detectable beyond the 4th serial dilution (1.25 μg/mL). Due to the fact that both double mutants maintain residual toxin activity, we generated triple mutants to include H35L (H35L/D45A/Y118F, H35L/R66C/E70C) for examination as potential vaccine candidates. We then repeated the RBC lysis assay to ensure the vaccine candidate mutants were completely detoxified as seen with the H35L single mutant. As shown in Fig. 3.3.1B, both triple mutants have no detectable lysis at all concentrations, making these suitable antigens for vaccine analysis.

3.2.2 Characterization of mutant Hla variants: Binding and Oligomerization Capacity

To evaluate the ability of mutant toxins to interact with host cells, *in vitro* translated ^{35}S radiolabeled Hla mutants were generated (Supp Fig. 3.7.2) and used to evaluate the effect of the mutations on toxin binding to rabbit RBCs. All mutants generated an appropriate amount of protein and were radiolabeled efficiently. Of note, the D45A/Y118F mutation did cause the toxin to spontaneously oligomerize as shown by the high molecular weight band at ~175 kDa. To ensure the same amount of radiolabeled monomeric toxin was used in each assay, the band intensity of the monomer was calculated and normalized to wild type monomer. Rabbit RBCs were incubated with [^{35}S] labeled toxin at room temperature for 5 minutes, washed and then the cellular fraction was resuspended in scintillation fluid and bound ^{35}S-toxin was read on a liquid scintillation counter. As expected, there was no difference in binding capability with the single H35L mutation compared to wild-type, however both triple mutants significantly reduced the ability of Hla to bind to rabbit RBCs with H35L/R66C/E70C having the most prominent reduction (Fig 3.3.2A). In addition, we tested the double mutants (D45A/Y118F and R66CE70C) without the H35L mutation and as expected this did not change the binding efficiency of either mutant (data not shown).

The ability of Hla mutant toxins to assemble into pores and the stability of the pores formed was also interrogated. To analyze mutant toxin oligomerization, ^{35}S radiolabeled mutant toxins were incubated with rabbit RBCs for one hour at room temperature followed by exposure to 37°C, 60°C, or 80°C. Samples were analyzed by SDS-PAGE and phosphorimaging. The presence of high molecular weight oligomers is indicative of pre-pore/pore formation on the rabbit RBC surface. An oligomer complex was detected for all mutant toxins, however, the band

intensity for the triple mutants was significantly reduced due to the overall binding defect ensued with these mutations (Fig. 3.3.2A, B). Previous studies have demonstrated that wild type toxin is SDS and heat stable up to 66°C, while mutations that disrupt oligomer stability have a reduced capacity to remain in the assembled pre-pore at 50°C [77]. As expected, all mutants have detectable ~33kDa monomeric bands (denoted by the arrow) at each temperature and ~175kDa oligomer bands at 37°C (denoted by Hla_7), while these bands are lost at 80°C (Fig. 2B). H35L has been previously demonstrated to lose oligomer stability above 50°C, however, all mutant oligomer complexes including H35L, were present at 60°C. This result for H35L is likely due to the high concentration of toxin used in this assay to accommodate for the significant loss of binding signal with the other mutants. Since the double mutants retain some ability to lyse cells, while H35L does not, suggests that these mutations do not appear to completely abolish the stability of the oligomer or pore formation.

3.3.3 Impact of mutants on Hla structure and stability

In collaboration with the Amarasinghe lab, we examined the structural stability of each mutant using a thermal shift assay (TSA). In brief, this assay measures the melting temperature of a protein, defined by the temperature at which there is 50% protein denaturation, thus hydrophobic residue exposure. This assay utilizes ThermoFluor SYPRO Orange dye which binds nonspecifically to hydrophobic residues and is quenched by water. As the temperature increases, proteins will become disordered, exposing hydrophobic residues, which results in an increase of SYPRO Orange binding and fluorescence [83,84]. As shown in Figure 3.3.3, wild-type Hla, H35L and H35L/R66C/E70C exhibit similar melting curves, reaching 50% denaturation at 61-63°C. In contrast, H35L/D45A/Y118F does not reach 50% denaturation until almost 80°C, however the dye is able to bind before the protein has been exposed to an increase in temperature. This data

suggests that the monomeric structures of H35L and H35L/R66C/E70C are not altered and remain compact or globular in overall structure, comparable to the wild-type toxin. H35L/D45A/Y118F appears to be more stable than the other proteins, however, dye binding at room temperature indicates that the structure is inherently more disordered. This finding is well-aligned with our prediction that D45A and Y118F mutations disengage the pre-stem from the cap domain, thereby exposing the hydrophobic surface on the cap domain in the monomeric form.

3.3.4 Antigens and adjuvants have differential protection against S. aureus skin infection

To address if these distinct antigen properties and interaction with ADAM10 influence the immune response and adjuvanticity, we utilized two different FDA-approved adjuvant formulations with each toxoid and immunized mice prior to *S. aureus* skin infection. The first adjuvant contains squalene/DL-α-tocopherol/polysorbate 80 (AS03-like) and the second contains alum/monophosphoryl lipid A (AS04-like), both of which have been demonstrated to increase the number of activated $CD11c^+$ dendritic cells in the draining lymph node which are the main driver of antigen-specific T-cell priming [85]. As seen in Figure 3.3.4, all vaccine candidates with both adjuvant formulations provide significant protection against *S. aureus* skin infection compared to the sham controls. However, the vaccine candidates formulated with the AS03-like adjuvant were overall more effective and significantly reduced the abscess and dermonecrosis lesions compared to the AS04-like formulation. Of the vaccine antigen candidates, mice immunized with H35L/D45A/Y118F exhibited the largest lesions in both formulations with the most prominent difference within the first 48 hours post-infection. In fact, the abscesses were over two-fold larger in the AS04-like formulation compared to the AS03-like formulation. This reduction in protection was also evident in the dermonecrotic lesions in the AS04-like

H35L/D45A/Y118F-immunized mice with almost a 2-fold increase in lesion size compared to the other vaccine candidates.

3.3.5 Analysis of antibody titers and neutralizing capability

Anti-Hla serum antibody EC50 titers from vaccinated mice indicated successful vaccination as all vaccine candidates with both adjuvant formulations had a significant increase in antibody response above adjuvant control. Of the serum antibody responses, toxoids in combination with the AS03-like formulation all generated higher antibody titers compared to toxoids in combination with the AS04-like formulation, with H35L/R66C/E70C reaching significance (Fig. 3.3.5A). Interestingly, H35L/R66C/E70C generated the most robust antibody response in the AS03-like formulation with about a 2-fold increase in antibody titer as compared to the other vaccine candidates. Serum collected from the vaccinated mice was also tested for Hla neutralizing capacity. Rabbit RBCs were incubated with serum for 1 hour and then treated with wild type toxin. H35L/R66C/E70C exhibited a remarkable toxin neutralizing capability as compared to the other vaccine candidates providing 50% protection at dilution 1:3200 (Fig. 3.3.5B). The neutralizing capacity was not as prominent in the AS04-like formulations, but the overall trend remained the same. Figure 3.3.5C shows a plot of serologic protection from Hla-induced rabbit red cell lysis as a function of anti-Hla serum EC50 titer from vaccinated mice. Though the AS03-like formulations with H35L and H35L/D45AY118F generated similar antibody titers, the neutralizing capacity was greatly reduced with H35L/D45A/Y118F as RBC lysis reaches nearly 50%. In contrast, H35L/R66C/E70C had nearly a two-fold higher EC50 antibody titer than H35L however these antigens provided similar neutralizing capacity in both formulations. The diminished antibody titer and neutralizing capacity was even more evident with AS04-like adjuvant in combination with H35L/D45A/Y118F resulting in 70% RBC lysis.

These plots highlight key differences in the antigen/adjuvant formulations on overall vaccine effectiveness.

3.3.6 *VavCre*$^{+/-}$ *bAdam10*$^{+}$ red blood cells are sensitized to Hla

The details of the toxin-receptor interaction interface have remained elusive as purified ADAM10 is unable to bind the toxin, likely related to a requirement for receptor conformational determinants that only exist when displayed in the host cell membrane. To address this biological challenge, we generated a transgenic mouse line with increased *Adam10* expression on the surface of red blood cells. We utilized an established mouse line that harbors a bovine *Adam10* transgene driven under a CAG promoter and crossed them to mice containing the cre recombinase under control of the mouse vav 1 oncogene (*Vav1*) promoter which results in hematopoietic expression of the downstream gene. Upon tissue specific Cre-mediated recombination, endogenous *Adam10* is knocked out and bovine *Adam10 (bADAM10)* is expressed only in hematopoietic and progenitor cells (Fig. 3.3.6A). As murine red blood cells natively have low surface expression of ADAM10, it was unclear if it would be possible to generate an ADAM10 knock-in model on this cell type. To examine this, red blood cells were isolated from *VavCre*$^{+/-}$ *bAdam10*$^{+}$ and control (*VavCre* negative) mice and treated with purified toxin. As shown in Figure 3.3.6B, red blood cells isolated from *VavCre*$^{+/-}$ *bAdam10*$^{+}$ mice were significantly more sensitive to toxin treatment as compared to red cells isolated from control mice. In addition, *VavCre*$^{+/-}$ *bAdam10*$^{+}$ red blood cells also showed a significant increase in toxin binding (Fig. 3.3.6C). This data demonstrates that mouse red blood cells can in fact express an increased amount of functional ADAM10 on their surface. Furthermore, this data confirms the membranes of *VavCre*$^{+/-}$ *bAdam10*$^{+}$ expressing red blood cells can be used to visualize the

Hla-ADAM10 complex in its native confirmation with techniques such as cryo-electron microscopy.

3.4 Discussion & Conclusion

The α-toxin or Hla has long been recognized as one of the most important virulence factors encoded by *S. aureus* as it plays a critical role in injury in both skin necrosis and lethal infections. Though *S. aureus* and α-toxin have accumulated nearly a century's-worth of valuable research, major challenges that have hindered the field include: 1) the exact mechanism of the transformation from the oligomeric structure into the pore remains elusive; 2) the complete toxin and receptor binding interface and confirmational determinants are unknown; 3) no vaccine strategy against multiple virulence factors, including the α-toxin, has been successful.

Recent data from our lab has provided valuable insight on the first two challenges. We have shown specific regions within the metalloprotease domain proximal to the active site as well as the catalytic activity of ADAM10 are necessary for toxin binding and function. Furthermore, recent studies by Seegar et al., demonstrated that the cysteine-rich domain partially occludes the active site within the metalloprotease domain when ADAM10 is in an inactive state. Based on these findings we hypothesized that the structural confirmation and the activity state of ADAM10 may influence toxin binding. It is tempting to speculate that Hla binding to the metalloprotease domain could alter the ADAM10 structure enough to displace the cysteine-rich domain, and thus trigger the ADAM10 sheddase activity characteristic of Hla intoxication.

The fact that purified ADAM10 and Hla do not interact in solution has made studying this interaction challenging. Recent identification of host receptors for several bacterial toxins

has proven the necessity of live cells for proper folding of the receptor in its native lipid environment [86]. In order to better understand the Hla and ADAM10 interaction, we proposed to use red blood cells as they are an attractive cell model to use for a few reasons. First, RBCs are simple cells with a well-defined surface protein profile. The use of red blood cells will thus provide the lipid membrane needed for native protein folding as well as make visualization of the Hla-ADAM10 complex more targeted. Furthermore, we can generate RBC ghosts where the cellular membrane is preserved but devoid of other cellular components such as hemoglobin, etc. Second, RBCs are less sensitive to Hla-mediated lysis due to the low surface expression of ADAM10. This allowed us to easily assess if the transgene knock-in system is viable in these cells. The increase in Hla binding with *VavCre*$^{+/-}$ *bAdam10*$^{+}$ RBCs compared to control RBCs demonstrated the transgene cassette expressed an increased amount of ADAM10 as expected (Fig 3.3.6B). In addition, we were also able to show this system is functional as RBCs with *bAdam10* expression are sensitized to Hla-mediated lysis (Figure 3.3.6B). Last, isolating RBCs from mice is relatively simple and does not require terminal procedures. Submandibular bleeds can be performed on consecutive days and provides plenty of cells to use in multiple assays.

We therefore predict that this cell model can be used for advanced microscopy techniques which will allow us to gain structural insight into the complex molecular actions that conclude with toxin pore formation and ADAM10 activation. Cryogenic electron microscopy (CryoEM) and cryoelectron tomography (CryoET) provide the capability of high-resolution imaging of the molecular dynamics of proteins and protein complexes. In fact, recent advances in hardware and software cryo microscopy technology allows for a larger range of molecular weights and imaging at molecular to near-atomic levels as well as more flexible sample conditions [87,88]. Briefly, both techniques take thousands of 2D images at all possible

perspectives of the sample in a frozen-hydrated state, which captures how it naturally exists in solution. These images then get compiled into a 3D model. CryoEM captures images of many different parts of the structure that are frozen in various orientations (face-up, face-down, tilted to the side, etc.) while CryoET captures sequential pictures of a single structure as it is slowly rotated or tilted along one axis. CryoET can also resolve ambiguity present in 2D projection images and is better suited to image single and/or flexible structures that are difficult to visualize with CryoEM [87,88]. Utilizing both techniques will provide unique insight to the Hla and ADAM10 complex as we will be able to visualize basic uniform structures and heterogenous/flexible components of the structures when they interact. Some challenges and limitations to these techniques include a significant amount of sample optimization and the number of images that can be taken at one time to preserve sample integrity. Managing beam dosage will be important especially when using CryoET since a single particle will be constantly exposed and can only tolerate a low electron dose before significant damage occurs to the structure.

The third major challenge hindering the field has been the development of a successful *S. aureus* vaccine. It has already been established in multiple preclinical studies that active vaccination targeting Hla provides protection against infection [77-82]. However, due to the critical role of the Hla-ADAM10 interaction in *S. aureus* disease, we wondered if this interaction influences immunogenicity. The vaccine candidates we evaluated were chosen based on mutations that would not only alter the Hla-ADAM10 interaction but also the tertiary structure of Hla. H35L is a well characterized detoxified mutant and has been previously used in vaccination studies with great success in various mouse models [78]. Furthermore, this mutation is not predicted to change the tertiary structure and does not interfere with the Hla-ADAM10 binding

interaction (Figure 3.3.2A). To create an opposite effect, we generated the D45A/Y118F and R66C/E70C variants. D45A/Y118F is predicted to significantly change the tertiary structure by disengaging the pre-stem from the cap domain. In theory this would expose the N-terminal amino latch as well as partially unfold the monomeric structure. R66C/E70C is predicted to affect the binding properties, therefore preventing the Hla-ADAM10 interaction which would keep the toxin soluble.

Before we could analyze these vaccine candidates *in vivo*, we needed to ensure these mutations would detoxify the proteins to be safely used as vaccine antigens. We utilized rabbit red blood cells as they are the most sensitive cell type to the toxin and classically used to determine hemolytic activity of the α-toxin. During our initial characterization of these mutants, we found that both D45A/Y118F and R66C/E70C retained some lytic ability at 10 μg/mL or higher concentrations. This is not surprising for variant R66C/E70C as the mutations located in the rim domain have not been demonstrated to impact oligomer or pore stability [32,57]. We were unsure if the pre-stem detached from the cap domain would affect the oligomer or pore stability, however, D45A/Y118F did retain some lytic ability at higher concentrations than 10 μg/mL (data not shown). In addition, both variants ensued significant binding defects compared to wild-type and H35L, with R66C/E70C having the most prominent defect, as expected. Though the binding efficiency was reduced, both variants still appeared to form oligomeric complexes on rabbit red blood cells. The fact that these mutants still retain some hemolytic activity and H35L does not, suggests that the oligomeric complexes in these variants are stable and therefore undergo pore formation. The binding defect seems to be the main driver for reduced hemolytic activity in R66C/E70C, however, since D45A/Y118F has an intermediate binding capability and the hemolytic activity is even more reduced, suggests that the oligomer complex may be less

stable with D45A and Y118F mutations. These results are consistent with the non-specific binding ability of the toxin at high concentrations. This is nicely demonstrated with the R66C/E70C variant as it significantly loses lytic activity as the toxin is serially diluted. Due to the above findings, we finalized the vaccine candidates to have H35L as a third mutation to completely inactive them without changing the structure or binding properties. As shown in Figure 3.3.2B, introducing H35L into these variants completed inactivated the toxins without affecting binding (double mutant compared to triple mutant binding data not shown).

Next, we examined the effects of these mutations on the stability and structure of the proteins in solution. Thermal shift assays measure the thermal denaturation profile of proteins, indicating at which conditions and temperatures proteins are less tightly folded. This methodology is classically used to analyze protein stability within different solutions as well as protein-ligand interactions [84]. One of our rationales for novel vaccine design is that the structure of the antigen may influence immunogenicity and/or adjuvanticity. Moreover, altering the ability of the toxin antigen to interact with the host receptor may also drive a different immune response. Both H35L and H35L/R66C/E70C mutations seem to preserve the native monomeric structure of the toxin as well have a similar denaturing profile. Interestingly, H35L/D45A/Y118F showed increased binding of the SYPRO Orange dye at room temperature, indicating the monomeric structure is very different from the wild type and other mutants. In addition, H35L/D45A/Y118F did not reach 50% denaturation until almost 80°C. Together, this data suggests that the D45A/Y118F mutations do in fact disengage the pre-stem, exposing hydrophobic residues and significantly changing the structure, while H35L and R66C/E70C mutations do not have an overall effect on the structure of the native monomer. Of note, D45A/Y118F was also observed to spontaneously oligomerize (Supp Fig. 3.7.2) as well as had a

higher propensity to precipitate in solution during purification, which is indicative of altered protein folding.

We hypothesized that the immune system may recognize these antigens differently due to the binding and structural changes and therefore potentially process and respond differently. We also utilized two distinct FDA-approved adjuvant formulations, GSK AS03-like and GSK AS04-like formulations, as the adjuvant properties combined with the differing mutant antigen properties may elicit different responses. Our data shows the following: 1) all vaccine candidates are highly effective in both adjuvant formulations against *S. aureus* skin infection compared to the sham controls; 2) adjuvating H35L and H35L/R66C/E70C in either formulation provides similar and the best protection; 3) H35L/R66C/E70C had the highest antibody titer and toxin neutralization capability; 4) antigen H35L/D45A/Y118F provides differential protection compared to H35L and H35L/R66C/E70C in both adjuvants. Interestingly, mice immunized with H35L/D45A/Y118F in the AS04-like formulation had significantly larger abscess and dermonecrotic lesions compared to the other antigens in both formulations. This phenotype is the most evident within the first 48 hours post infection, however, the abscesses remained larger compared to the H35L and H35L/R66C/E70C abscesses throughout the duration of the experiment. In addition, the dermonecrotic lesions were significantly larger, measuring up to 20mm^2 where the other antigens maximum measurements stayed under 10-15mm^2 in both formulations.

Clinically speaking, all antigens and adjuvant combinations provide efficient protection against S. aureus skin infection, however, the antibody titers and neutralization capability of each of the antigens highlighted the discrepancies in the elicited immune response. The mutants

adjuvanted with the AS03-like formulations overall produced a more robust antibody response as the EC50 titers of each antigen are 2-fold higher than in the AS04-like formulation. Furthermore, H35L/R66C/E70C also had a 2-fold higher antibody titer compared to the other antigens. The overall toxin neutralizing capability of the antigens combined with the AS03-like formulations were overall higher than the AS04-like formulations. H35L/R66C/E70C showed a remarkable neutralizing capability as the serum could be diluted 34-fold more than H35L serum and 658-fold more than H35L/D45A/Y118F serum and still provide 50% toxin neutralization.

Both H35L and H35L/R66C/E70C performed similarly and were overall the more effective vaccine candidates, in spite of their differences in receptor binding properties. In addition, H35L/D45A/Y118F retains some binding to the host receptor but the monomeric structure is structurally less compact and behaves very differently compared to wild-type Hla, H35L or H35L/R66C/E70C. Furthermore, H35L/D45A/Y118F spontaneously oligomerizes which may also impact immunogenicity due to the toxin aggregates potentially covering useful epitopes. We also have preliminary data that showed Hla mutants adjuvanted with the AS03-like formulation overall induced a better $CD4^+$ memory T cell response, with H35L/R66C/E70C inducing even more of these cells compared to all other antigens. Furthermore, mice that received AS03-like sham immunizations overall had larger lesions than mice that received AS04-like sham immunizations, suggesting that AS03-like adjuvants are potent immune stimulators. Together this data suggests that the host immune response is recognizing and processing these antigens differently and responding more effectively in combination with the AS03 formulation.

It is possible that the H35L/R66C/E70C antigen may elicit a more robust immune response by virtue of its ability to preserving the native monomeric structure of the toxin while rendering it unable to bind to the host receptor. Based on all data available to date, we made the following hypotheses: 1) a soluble antigen may lead to more antigen available within the tissue microenvironment to get taken up and processed specifically by professional antigen presenting cells; 2) the Hla-ADAM10 complex may play a role in how the host immune system recognizes and processes the antigen; 3) toxin mutant antigens that preserve native structure of the toxin may be important for useful epitope recognition. The increased antibody titer and CD4 memory T cell response observed with antigen H35L/R66C/E70C may be the result of more soluble antigen available for internalization specifically by professional APCs via endocytic pathways. For example, dendritic cells constitutively use macropinocytosis to sample the local environment in order to initiate the adaptive immune response through MHC-II antigen presentation to $CD4^+$ T cells. While the H35L antigen provides similar protection against *S. aureus* skin infection to H35L/R66C/E70C, the antibody titer, neutralizing capability and $CD4^+$ T memory response were significantly lower. The cause of this reduction could be two-fold: first, H35L antigen binds to ADAM10, which is on almost every cell type and therefore may reduce the available antigen to be taken up by professional APCs. Thus, ADAM10 expression on non-professional APCs and other cells such as the keratinocytes or epithelial cells could be acting as an 'antigen sink'. Second, antigen bound to ADAM10 taken up by these other cells would most likely be processed and presented through MHC-I to activated $CD8^+$ T cells rather than $CD4^+$ T cells, which could explain the decrease in antibody response. Furthermore, it is interesting to speculate that the Hla-ADAM10 complex could be internalized together and processed more like a self-antigen through normal membrane recycling pathways and reduce the amount of Hla antigen properly presented.

One way we could test if a soluble Hla antigen is more effective than a cell bound Hla antigen, is by immunizing wild-type and ADAM10$^{-/-}$ mice with H35L. The loss of ADAM10 expression in the ADAM10$^{-/-}$ would result in soluble H35L and may improve antibody responses compared to wild-type H35L immunized mice.

In conclusion, our studies have demonstrated that immunization with three distinct candidate vaccine antigens provided significant protection against *S. aureus* skin infection yet elicited distinguishable immune responses. Not only did the structural and binding properties of the Hla antigens play a role but the type of adjuvant used in combination with the antigens impacted vaccine efficacy. Our lab has previously shown that Hla hampers the T cell response, utilizing an antigen that elicits a high neutralizing capability like H35L/R66C/E70C could be the key to preserving the T cell compartment. These studies could provide valuable insight not only for vaccine design but also shed light on how bacterial toxins that bind host receptors are recognized and processed differently than other antigens. Lastly, we have generated an ADAM10 knock-in system on mouse red blood cells that will allow us to visualize the Hla-ADAM10 complex for the first time through advanced microscopy techniques. Identifying the exact mechanism and structural interface between the toxin and receptor would provide important implications for therapeutic approaches and could provide greater insight on the biologic function of pore-forming toxins in general.

3.5 Materials and Methods

Plasmid Construction and Hla Antigen Purification

Toxin variants (double and triple mutants) were cloned into the pET24b expression vector containing a C-terminal polyhistidine tag. PCR products were amplified from Hla template from DNA constructs previously generated in the Bubeck Wardenburg lab. Vector and mutant insert ligation reactions were transformed into *Escherichia coli* DH5 alpha, colonies screened for positive clones and each construct sequenced for verification. Confirmed clones were then transformed into *E. coli* BL21 for recombinant protein expression and purification. Generation of recombinant polyhistidine-tagged wildtype Hla and HlaH35L (H35L) have been described previously [77]. Recombinant toxin variants were prepared and purified using standard protocols, LPS extracted and evaluated by 10% SDS-polyacrylamide gel electrophoresis (PAGE) followed by Coomassie blue staining.

Hla activity assay (rRBC hemolysis)

Rabbit red blood cell (rRBC) hemolysis was assayed by incubation of rRBCs (Hemostat Labs) with purified toxin variants ranging from 300-0.14 nM for 1 hour at room temperature. Following incubation, cells were pelleted by centrifugation and supernatant absorbance at 450nm measured. Percent rRBC hemolysis were calculated relative to 1% Triton X-100 maximal lysis controls. The assays were performed in triplicate and repeated for reproducibility on separate days.

rRBC binding and oligomerization assays

Radiolabeled Hla was synthesized by *in vitro* transcription and translation in an *E. coli* S30 extract (Promega) supplemented with T7 RNA polymerase, rifampin (rifampicin), and [^{35}S] methionine according to the manufacturer's instructions. For the binding assay, one hundred

twenty microliters of 12.5% rabbit red blood cells (rRBC) in K-PBSA/βME (20 mM potassium phosphate [monobasic], 150 mM NaCl [pH 7.4], 1 mg/ml bovine serum albumin, 1 mM β-mercaptoethanol) was incubated with 10 µl of radiolabeled Hla mixture for 5 minutes at room temperature. Cells were pelleted, washed twice with ice-cold PBS, resuspended in 200µl of PBS and added to scintillation fluid. Radioactivity from cell bound toxin was quantified on a Beckman LS6000 scintillation counter. For oligomerization assays, rRBCs were used as described above but incubated with 30 µl of the radiolabeled Hla mixture (~ 1 nM) for 1 h at room temperature. Following incubation, cells were pelleted and washed with 500 µl K-PBSA/βME and then resuspended in 90 µl 1× Laemmli buffer. Samples were divided into 30 µl aliquots and incubated at 37°C, 60°C and 80°C for 10 min before samples were loaded onto 10% sodium dodecyl sulfate (SDS)-polyacrylamide gel electrophoresis (PAGE) gels for electrophoresis. The gels were dried, and then the results were visualized using a phosphorimager. Binding assays were performed in triplicate and repeated for reproducibility on separate days. Oligomerization assays were performed with a single replicate and repeated for reproducibility on separate days.

Thermal Shift Assay

The stability of protein was measured by the melting temperature of each protein (50% denaturation point). Each well contained a final concentration of 5 µM protein, 4.5 × Sypro Orange, and 1x buffer (20 mM Tris pH 7.5, 150 mM NaCl). The plates were heated in StepOnePlus™ Real-Time PCR System (Thermo Fisher) from 20 to 90 °C in increments of 0.3°C. The wavelengths for excitation and emission were 490 and 575 nm, respectively.

Immunization and S. aureus skin infection

All animal experiments were reviewed, approved, and supervised by the Institutional Animal Care and Use Committee (IACUC) at Washington University at St. Louis. Hla antigens were LPS extracted and prepared with either AS03-like adjuvant formulation, 1:1 antigen to AddaS03 (InvivoGen, Cat # 10253-42-02) or AS04-like formulation with antigen plus 500 μg/mL Alhydrogel (InvivoGen, cat# vac-alu-250) and 50 μg/mL of MPLA-SM VacciGrade (InvivoGen, cat# vac-mpla). 20 micrograms of each antigen were delivered intramuscularly to cohorts of ten 3-week-old C57BL/6 male mice (Jackson Laboratory) on days 0 and 14. For SSTI modeling, on day 21 mice were anesthetized via intraperitoneal injection of ketamine (20 mg/kg) and xylazine (5 mg/kg) followed by right flank subcutaneous challenge with $1x10^8$ CFU S. aureus strain USA300/LAC in 50 μL PBS [71]. Lesional abscess and dermonecrosis area (mm2) was measured at 24-hour intervals for 7 days. Abscess and dermonecrosis size was determined according to the formula $A=(\pi/2)(\text{length mm})(\text{width mm})$ [42,79]. Naïve serum was collected from 5 mice on day 0 and 14 prior to *S. aureus* challenge to determine antibody titers following immunization.

ELISA and Antibody Neutralization Assays

Sera collected from immunized mice was diluted 1:25 and then four-fold serial dilutions for eight dilutions total. Anti-Hla titers were determined by ELISA as previously described[78] and ELISA absorbance readings (450nm) used for generation of four-parameter log(dose)-response curves using Prism software. For the neutralization assay, the serum was diluted 1:100 and then two-fold for eight dilutions total. The diluted serum was incubated with toxin for 15 minutes at room temperature before $2.5x10^8$ c/ml of rabbit red cells were added. The final concentration of toxin was 2nM and the assay incubated at room temperature for 1 hour. Cells were pelleted and supernatant absorbance readings (450nm) were used to generate non-linear regression curves

with log (inhibitor) vs. response – variable slope curves using GraphPad Prism software. Both the ELISA and neutralization assays were performed in triplicate.

Generation of VavCre$^{+/-}$ *bAdam10*$^{+}$ mice

Mice harboring the bovine *Adam10* transgene were generated using a Cre-inducible knock-in system. The transgenic cassette includes a CAG promoter followed by *LoxP* flanked *eGFP* and a bovine poly-adenosine site. *eGFP* cDNA and the poly-adenosine site will be excised upon Cre recombination and allow the dormant transgene to be expressed (Fig. 3.3.6A). Bovine Adam10 constructs were generated by PCR and include a carboxyl-terminus human influenza hemagglutinin tag. The construct was sequence confirmed using bovine Adam10 primers and prepared according to instructions by the Transgenic Mouse and Embryonic Stem Cell Facility at The University of Chicago for ES injection. F0 progeny were screened for the presence of the bovine Adam10 transgene via GFP signal using a BlueStar Flashlight (NightSea). F0 males and females expressing GFP were crossed to C57BL6 mice to generate F1 progeny. F1 mice were then crossed to homozygous Adam10 floxed allele mice (*Adam10*$^{loxP/loxP}$). Progeny were screened by PCR for the Adam10 floxed allele and for the presence of GFP. Mice heterozygous for the Adam10 floxed allele and positive for the bovine Adam10 transgene were crossed to generate homozygous *Adam10* floxed and bovine Adam10 transgene positive mice (*Adam10*$^{loxP/loxP}$*/bAdam10).* Tissue-specific experimental mice utilized in the mouse red blood cells isolation studies were generated by crossing *Adam10*$^{loxP/loxP}$*/bAdam10* mice to Vav-Cre (The Jackson Laboratory). Mice were then screened for Vav-Cre and the b*Adam10* transgene cassette (*VavCre*$^{+/-}$ *bAdam10*$^{+}$*).*

VavCre$^{+/-}$ *bAdam10*$^{+}$ mouse red blood cells

Blood isolation: Whole blood was collected by submandibular puncture using 5 mm Goldenrod Animal Lancets and diluted with five mLs of PBS. To isolate the red blood cells, the whole blood was centrifuged at 500xg for 10 minutes and washed three times with PBS. The red blood cells were then resuspended in PBS, counted and diluted to the necessary concentration for the assays. For the hemolysis assay, $2.5x10^8$ cells/mL were incubated with 2nM of purified Hla toxin for 1 hour at room temperature. Following incubation, cells were pelleted by centrifugation and supernatant absorbance 450nm was measured. Percent RBC hemolysis were calculated relative to 1% Triton X-100 maximal lysis controls. For the radiolabeled binding assay, $5x10^8$ cells were incubated for 5 minutes at room temperature with approximately 1 nM of [^{35}S] methionine-radiolabeled toxin and performed as described above. The assays were performed in triplicate and repeated for reproducibility on separate days.

Statistical analysis

Statistical analysis was performed on GraphPad Prism software using one-way ANOVA with Tukey's multiple comparison test, significance level 0.05. Assessment of statistical significance in skin infection studies was performed on GraphPad Prism software using Multiple unpaired T tests, $p < 0.05$.

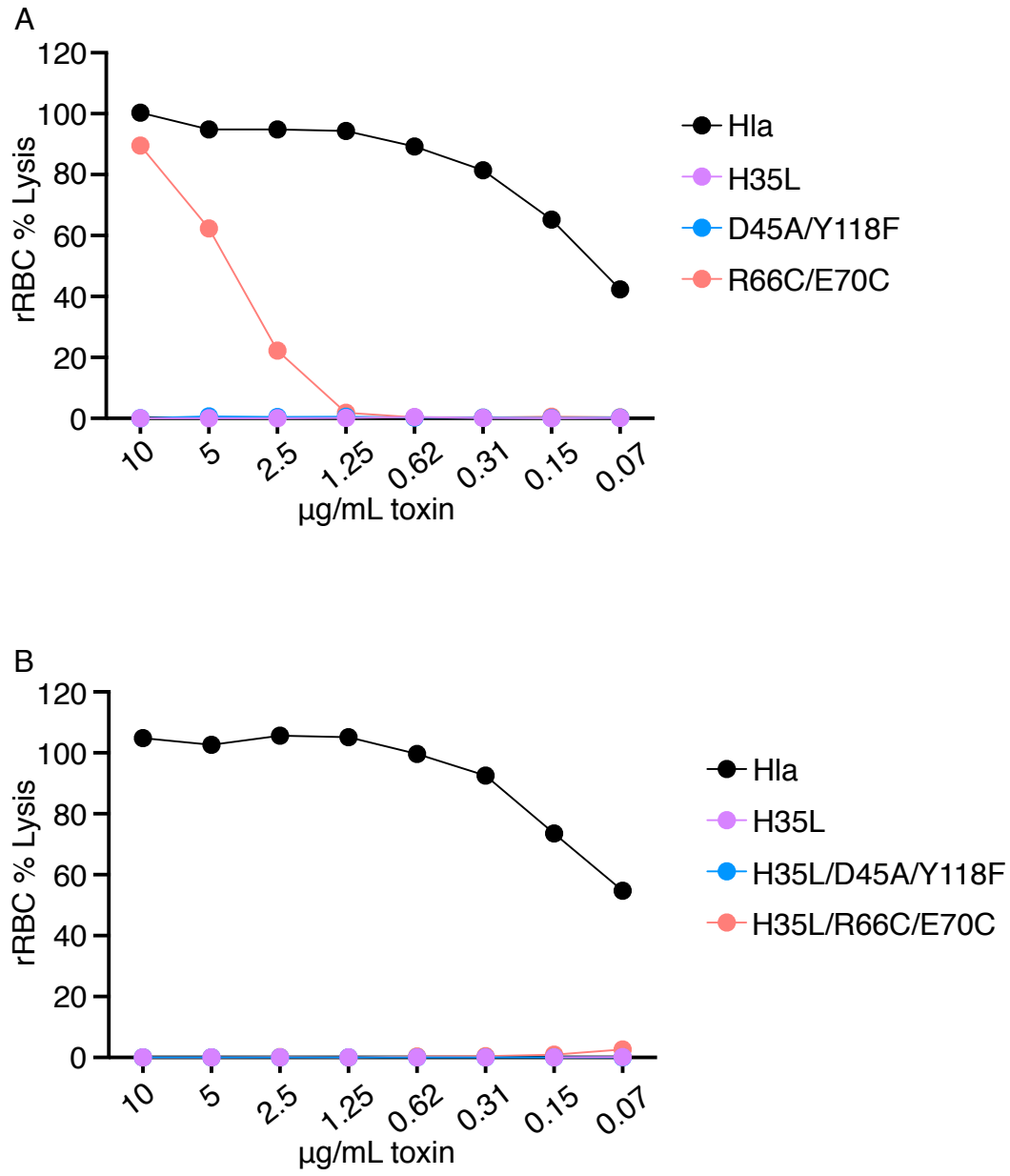

Figure 3.3.1: Hla mutant characterization: rRBC Lysis

Activity of Hla double (A) and triple (B) mutant variants was assessed via rabbit RBC lysis. Rabbit RBCs were incubated across a range of toxin concentrations for one hour at room temperature. Absorbance at 475nm of reaction supernatants was measured and percent lysis was calculated relative to detergent maximal lysis controls (0.1% Triton X-100).

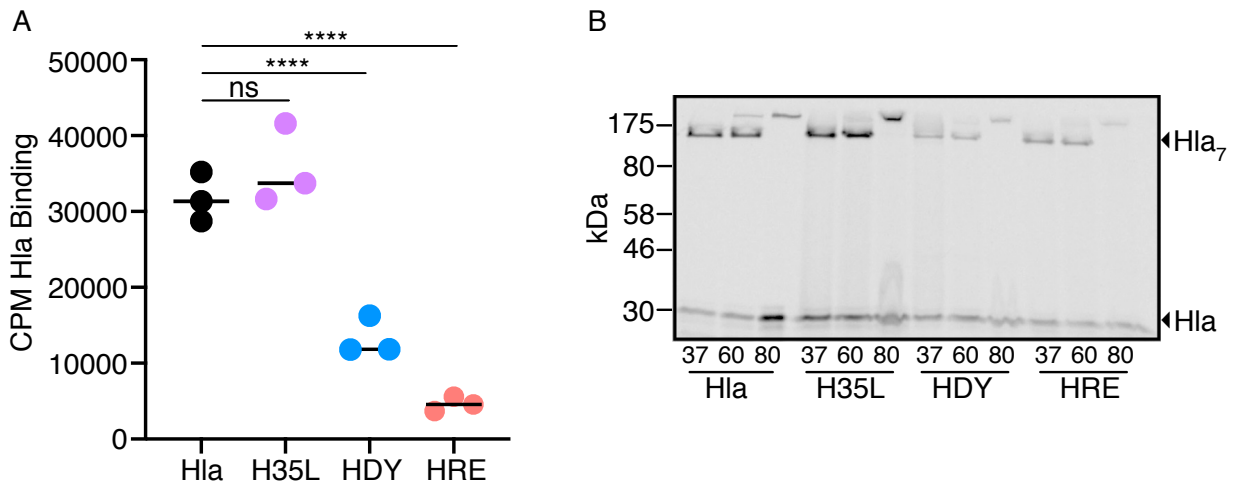

Figure 3.3.2. Hla mutant characterization: Binding and Oligomerization Capacity

* Mutant abbreviations are as follows: HDY (H35L/D45A/Y118F), HRE (H35L/R66C/E70C).

A. Each toxin variant was assessed for the binding capacity to rRBCs. Each toxin was incubated with rRBCs cells for 5 minutes, pelleted, supernatants removed and radiolabeled toxin in the cellular fraction assessed by detection of ^{35}S cpm. One-way ANOVA with Tukey's multiple comparison test was performed using GraphPad Prism software, $p < 0.05$.
B. Toxin pore assembly, formation, and stability was examined for each variant. ^{35}S radiolabeled mutant toxins were incubated with rabbit RBCs for one hour at room temperature followed by additional incubation at 37°C, 60°C, or 80°C for 10 minutes. Samples were separated by SDS-PAGE followed by phosphor-imaging for detection of high molecular weight oligomers. Toxin monomers are denoted by the arrow and toxin oligomers denoted by Hla_7.

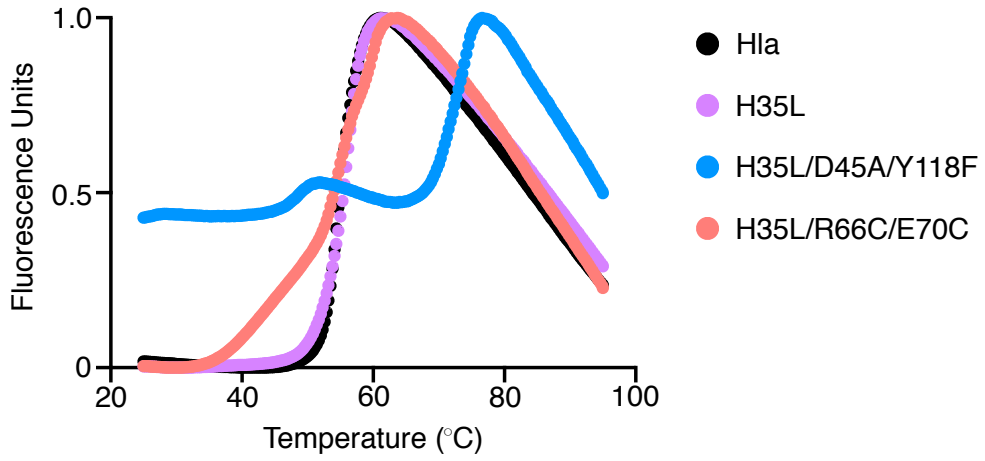

Protein	Melting Temperature (°C)
Hla	61.58
H35L	61.92
H35L/D45A/Y118F	76.90
H35L/R66C/E70C	63.84

Figure 3.3.3: Structural and stability analysis

The structural changes and stability of each toxin variant was compared to the wild-type toxin. Five µM of each mutant was incubated with Sypro Orange dye and assay buffer. The melting curves and Melting Temperatures (table) was measured by heating the plates in a StepOnePlus™ Real-Time PCR System (Thermo Fisher) from 20 to 90 °C in increments of 0.3°C. The wavelengths for excitation and emission were 490 and 575 nm, respectively.

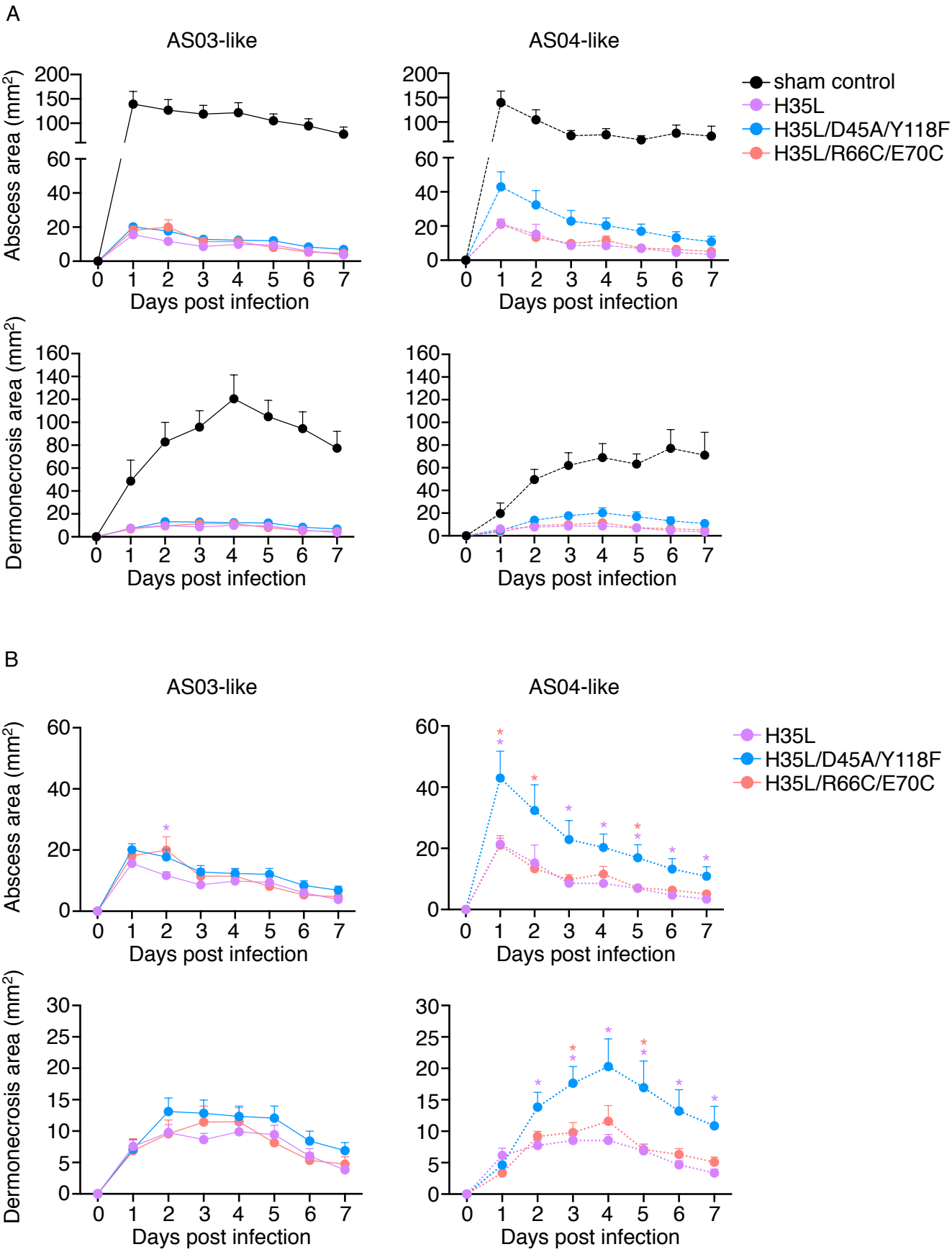
A
AS03-like
AS04-like
Abscess area (mm²)
Dermonecrosis area (mm²)
Days post infection
sham control
H35L
H35L/D45A/Y118F
H35L/R66C/E70C
B
AS03-like
AS04-like
Abscess area (mm²)
Dermonecrosis area (mm²)
Days post infection
H35L
H35L/D45A/Y118F
H35L/R66C/E70C

Figure 3.3.4: Hla mutants and adjuvants provide differential vaccine protection

Mice were vaccinated with Hla variants H35L, H35L/D45A/Y118F, H35L/R66C/E70C or adjuvants alone and challenged subcutaneously with $1x10^8$ *S. aureus* strain USA300. The left panels of figures A and B represent immunizations with AS03-like formulations (solid lines), the right side of both figures represent immunizations with AS04-like formulations (dotted lines). Lesion abscess and dermonecrosis area was measured at 24-hour intervals for 7 days. Figure A includes the sham controls and Figure B only includes immunized groups with statistical analyses. Multiple unpaired T tests were performed on GraphPad Prism software, $p < 0.05$. Asterisks show significant differences comparing H35L/D45A/Y1118F (aqua) to H35L (lavender) and H35L/R66C/E70C (orange).

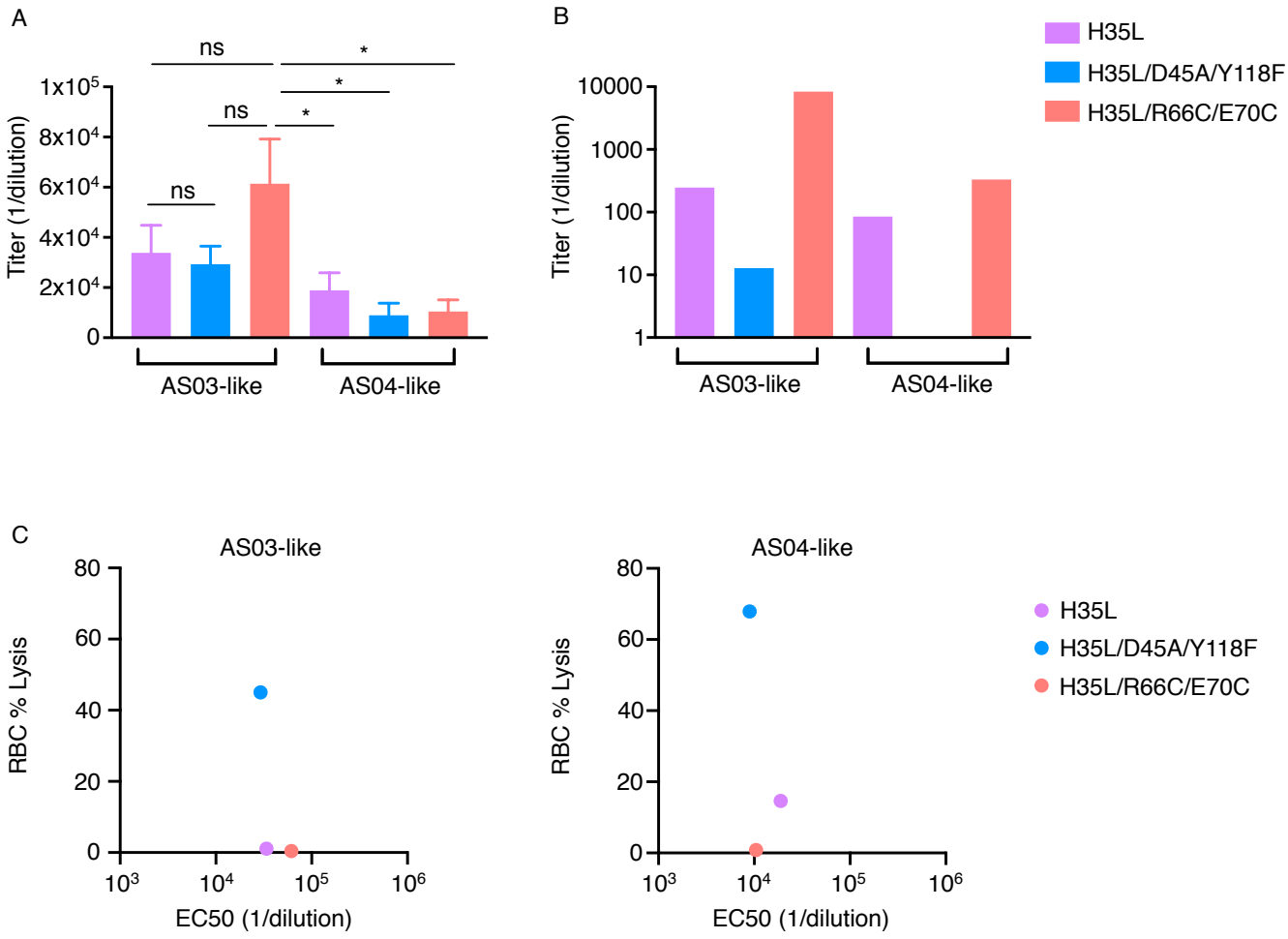

Figure 3.3.5: Antibody titers and neutralization

A. Naïve serum was collected on days 0 and 14 prior to infection and Hla ELISAs performed with serially diluted sera. ELISA absorbance readings were used to generate four-parameter log(dose)-response curves using Prism software for EC50 titer extrapolation. One-way ANOVA was performed with GraphPad Prism software using Tukey's multiple comparison test, $p < 0.05$.
B. To determine toxin neutralization capacity of the serum, toxin was incubated with serially diluted sera for 1 hour at room temperature and then added to rRBCs. Absorbance at 475nm of reaction supernatants was measured and percent lysis was calculated relative to detergent maximal lysis controls (0.1% Triton X-100). Absorbance readings were used to generate four-parameter log(dose)-response curves using Prism software for EC50 titer extrapolation.
C. Plot of serologic protection from Hla-induced rabbit red cell lysis as a function of anti-Hla serum EC50 titer from vaccinated mice.

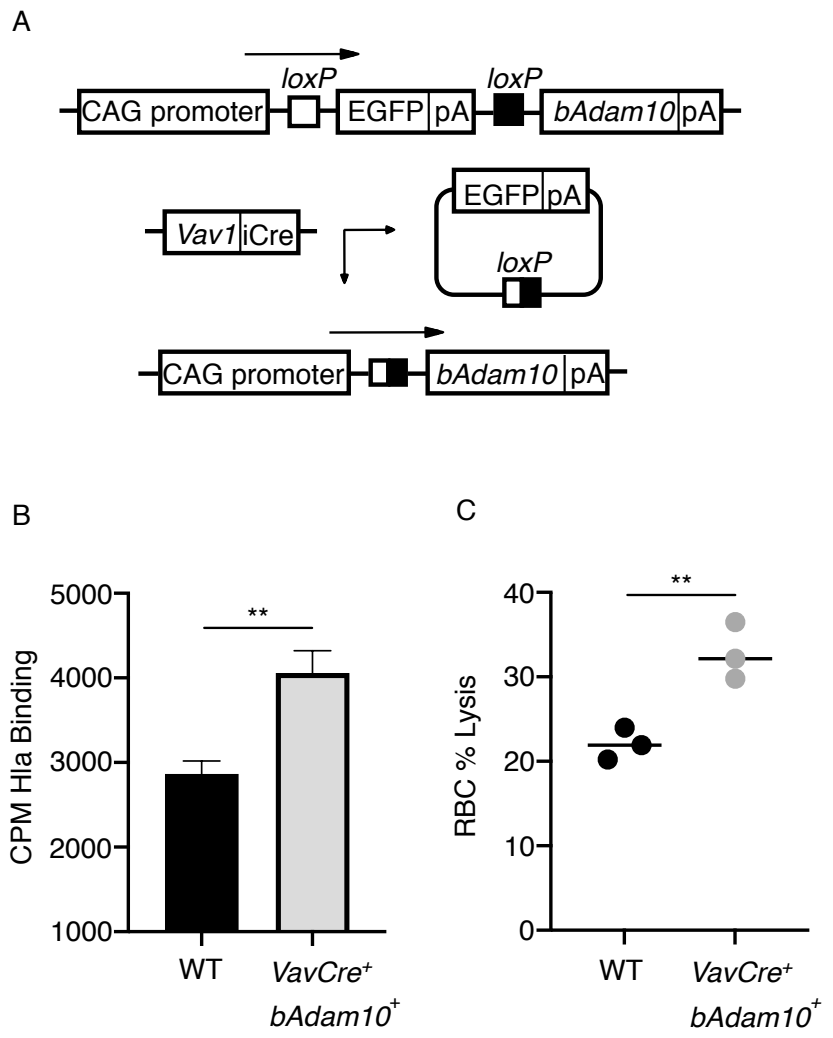

Figure 3.3.6 *VavCre*$^{+/-}$ *bAdam10*$^{+}$ mouse red blood cells are sensitized to Hla

A. Genetic strategy to generate mice harboring a Cre-induced deletion of endogenous mouse *Adam10* and Cre-inducible knock-in of *bAdam10* in hematopoietic and progenitor cells using a *Vav1* promoter-driven Cre recombinase.
B. Red blood cells isolated from *VavCre*$^{+/-}$ *bAdam10*$^{+}$ and control mice were assessed for the binding of [^{35}S] radiolabeled Hla toxin. Cells were incubated for 5 minutes with radiolabeled toxin at room temperature. Cells were washed and pelleted, supernatants removed and radiolabeled toxin in the cellular fraction assessed by detection of ^{35}S cpm.
C. Red blood cells isolated from *VavCre*$^{+/-}$ *bAdam10*$^{+}$and control mice were assessed for the Hla toxin sensitivity. Cells were incubated with toxin for 1 hour at room temperature. Absorbance at 475nm of reaction supernatants was measured and percent lysis was calculated relative to detergent maximal lysis controls (0.1% Triton X-100).

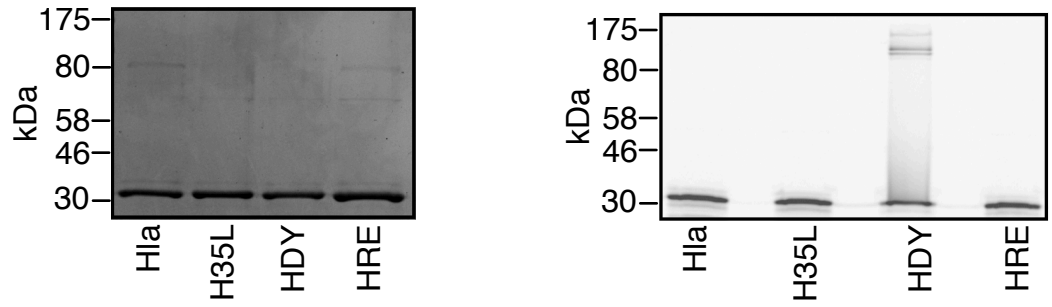

Supplemental Figure 3.7.1: Purified Hla mutants

(Left panel) Purified Hla proteins were separated by 10% SDS-PAGE and stained with InstantBlue coomassie stain for 15 minutes to confirm protein size and purity.

Supplemental Figure 3.7.2: [^{35}S] methionine labeled Hla mutants

(Right panel) [35S] methionine labeled Hla toxins were generated using *in vitro* transcription and translation. Toxins were separated by 10% SDS-PAGE and developed by phoshorimaging to confirm protein size and purity.

* Mutant abbreviations are as follows: HDY (H35L/D45A/Y118F), HRE (H35L/R66C/E70C)

References

1. Tong, S. Y., Davis, J. S., Eichenberger, E., Holland, T. L., & Fowler, V. G. (2015). Staphylococcus aureus infections: Epidemiology, pathophysiology, clinical manifestations, and management. Clinical Microbiology Reviews, 28(3), 603-661. https://doi.org/10.1128/cmr.00134-14

2. Lowy, F. D. (1998). Staphylococcus aureus Infections. New England Journal of Medicine, 339(8), 520-532. https://doi.org/10.1056/nejm199808203390806

3. Ogston, A. (1984). "On abscesses". Clinical Infectious Diseases, 6(1), 122-128. H ttps://doi.org/10.1093/clinids/6.1.122

4. Adhikari, R. P. (2021). Staphylococcal infections: Host and pathogenic factors. Microorganisms, 9(5), 1080. https://doi.org/10.3390/microorganisms9051080

5. David, M. Z., & Daum, R. S. (2010). Community-associated methicillin-resistant staphylococcus aureus: Epidemiology and clinical consequences of an emerging epidemic. Clinical Microbiology Reviews, 23(3), 616-687. https://doi.org/10.1128/cmr.00081-09

6. David, M. Z., & Daum, R. S. (2017). Treatment of staphylococcus aureus infections. Current Topics in Microbiology and Immunology, 325-383. https://doi.org/10.1007/82_2017_42

7. Noskin, G. A., Rubin, R. J., Schentag, J. J., Kluytmans, J., Hedblom, E. C., Jacobson, C., Smulders, M., Gemmen, E., & Bharmal, M. (2007). National trends in staphylococcus aureus infection rates: Impact on economic burden and mortality over a 6-Year period (1998-2003). Clinical Infectious Diseases, 45(9), 1132-1140. https://doi.org/10.1086/522186

8. Miller, L. S., Fowler, V. G., Shukla, S. K., Rose, W. E., & Proctor, R. A. (2019). Development of a vaccine against staphylococcus aureus invasive infections: Evidence based on human immunity, genetics and bacterial evasion mechanisms. FEMS Microbiology Reviews, 44(1), 123-153. https://doi.org/10.1093/femsre/fuz030.

9. Kourtis, A. P., Hatfield, K., Baggs, J., Mu, Y., See, I., Epson, E., Nadle, J., Kainer, M. A., Dumyati, G., Petit, S., Ray, S. M., Ham, D., Capers, C., Ewing, H., Coffin, N., McDonald, L. C., Jernigan, J., & Cardo, D. (2019). Vital Signs: Epidemiology and recent trends in methicillin-resistant and in methicillin-susceptible staphylococcus aureus Bloodstream infections — United States. MMWR. Morbidity and Mortality Weekly Report, 68(9), 214-219. https://doi.org/10.15585/mmwr.mm6809e1

10. Proctor, R. A. (2012). Is there a future for a staphylococcus aureus vaccine? Vaccine, 30(19), 2921-2927. https://doi.org/10.1016/j.vaccine.2011.11.006

11. Archer, N. K., Harro, J. M., & Shirtliff, M. E. (2013). Clearance of staphylococcus aureus nasal carriage is T cell dependent and mediated through Interleukin-17A expression and neutrophil influx. Infection and Immunity, 81(6), 2070-2075. https://doi.org/10.1128/iai.00084-13

12. Proctor, R. A. (2012). Challenges for a universal staphylococcus aureus vaccine. Clinical Infectious Diseases, 54(8), 1179-1186. https://doi.org/10.1093/cid/cis033

13. Lacey, K., Geoghegan, J., & McLoughlin, R. (2016). The role of staphylococcus aureus virulence factors in skin infection and their potential as vaccine antigens. Pathogens, 5(1), 22. https://doi.org/10.3390/pathogens5010022.

14. Spaan, A., Henry, T., Van Rooijen, W., Perret, M., Badiou, C., Aerts, P., Kemmink, J., De Haas, C., Van Kessel, K., Vandenesch, F., Lina, G., & Van Strijp, J. (2013). The staphylococcal toxin Panton-Valentine Leukocidin targets human C5a receptors. Cell Host & Microbe, 13(5), 584-594. https://doi.org/10.1016/j.chom.2013.04.006

15. Powers, M. E., & Wardenburg, J. B. (2014). Igniting the fire: Staphylococcus aureus virulence factors in the pathogenesis of sepsis. PLoS Pathogens, 10(2), e1003871. https://doi.org/10.1371/journal.ppat.1003871

16. Kozlowski, L. M., Lambris, J. D., & Levinson, A. I. (2008). Effect of a putative B cell Superantigen on complement. Annals of the New York Academy of Sciences, 764(1), 356-358. https://doi.org/10.1111/j.1749-6632.1995.tb55846.x

17. Cheung, G. Y., Bae, J. S., & Otto, M. (2021). Pathogenicity and virulence of staphylococcus aureus. Virulence, 12(1), 547-569. https://doi.org/10.1080/21505594.2021.1878688

18. Seilie, E. S., & Bubeck Wardenburg, J. (2017). Staphylococcus aureus pore-forming toxins: The interface of pathogen and host complexity. Seminars in Cell & Developmental Biology, 72, 101-116. https://doi.org/10.1016/j.semcdb.2017.04.003

19. Berube, B., & Wardenburg, J. (2013). Staphylococcus aureus α-toxin: Nearly a century of intrigue. Toxins, 5(6), 1140-1166. https://doi.org/10.3390/toxins5061140

20. Glenny, A. T., & Stevens, M. F. (1935). Staphylococcus toxins and antitoxins. The Journal of Pathology and Bacteriology, 40(2), 201-210. https://doi.org/10.1002/path.1700400202

21. Bhakdi, S., & Tranum-Jensen, J. (1991). Alpha-toxin of staphylococcus aureus. Microbiological Reviews, 55(4), 733-751. https://doi.org/10.1128/mr.55.4.733-751.1991

22. Bigger, J. W. (1937). Pathogenic staphylococci. BMJ, 2(4008), 837-841. https://doi.org/10.1136/bmj.2.4008.837

23. Siegel, I., & Cohen, S. (1964). Action of Staphylococcal Toxin on Human Platelets. Journal of Infectious Diseases, 114(5), 488–502. https://doi.org/10.1093/infdis/114.5.488

24. Füssle, R., Bhakdi, S., Sziegoleit, A., Tranum-Jensen, J., Kranz, T., & Wellensiek, H. J. (1981). On the mechanism of membrane damage by staphylococcus aureus Alpha-toxin. Journal of Cell Biology, 91(1), 83-94. https://doi.org/10.1083/jcb.91.1.83

25. Walker, B., Krishnasastry, M., Zorn, L., Kasianowicz, J., & Bayley, H. (1992). Functional expression of the alpha-hemolysin of Staphylococcus aureus in intact Escherichia coli and in cell lysates. Deletion of five C-terminal amino acids selectively impairs hemolytic activity. Journal of Biological Chemistry, 267(15), 10902–10909. https://doi.org/10.1016/S0021-9258(19)50103-X

26. Tweten, R. K., Christianson, K. K., & Iandolo, J. J. (1983). Transport and processing of staphylococcal Alpha-toxin. Journal of Bacteriology, 156(2), 524-528. https://doi.org/10.1128/jb.156.2.524-528.1983

27. Song, L., Hobaugh, M. R., Shustak, C., Cheley, S., Bayley, H., & Gouaux, J. E. (1996). Structure of staphylococcal α-hemolysin, a Heptameric Transmembrane pore. Science, 274(5294), 1859-1865. https://doi.org/10.1126/science.274.5294.1859

28. Menestrina, G., Dalla Serra, M., & Prévost, G. (2001). Mode of action of β-barrel pore-forming toxins of the staphylococcal α-hemolysin family. Toxicon, 39(11), 1661-1672. https://doi.org/10.1016/s0041-0101(01)00153-2

29. Gray, G. S., & Kehoe, M. (1984). Primary sequence of the Alpha-toxin gene from staphylococcus aureus wood 46. Infection and Immunity, 46(2), 615-618. https://doi.org/10.1128/iai.46.2.615-618.1984

30. Tobkes, N., Wallace, B. A., & Bayley, H. (1985). Secondary structure and assembly mechanism of an oligomeric channel protein. Biochemistry, 24(8), 1915–1920. https://doi.org/10.1021/bi00329a017

31. Gouaux, J. E., Braha, O., Hobaugh, M. R., Song, L., Cheley, S., Shustak, C., & Bayley, H. (1994). Subunit stoichiometry of staphylococcal Alpha-hemolysin in crystals and on membranes: A heptameric transmembrane pore. Proceedings of the National Academy of Sciences, 91(26), 12828-12831. https://doi.org/10.1073/pnas.91.26.12828

32. Galdiero, S., & Gouaux, E. (2004). High resolution crystallographic studies of α-hemolysin-phospholipid complexes define heptamer-lipid head group interactions: Implication for understanding protein-lipid interactions. Protein Science, 13(6), 1503-1511. https://doi.org/10.1110/ps.03561104

33. Jenul, C., & Horswill, A. R. (2019). Regulation of Staphylococcus aureus Virulence. Microbiology Spectrum, 7(2). https://doi.org/10.1128/microbiolspec.GPP3-0031-2018

34. Novick, R. P., Ross, H. F., Projan, S. J., Kornblum, J., Kreiswirth, B., & Moghazeh, S. (1993). Synthesis of staphylococcal virulence factors is controlled by a regulatory RNA molecule. The EMBO Journal, 12(10), 3967–3975. https://doi.org/10.1002/j.1460-2075.1993.tb06074.x

35. McNiven, A. C., & Arbuthnott, J. P. (1972). Cell-associated Alpha-toxin from staphylococcus aureus. Journal of Medical Microbiology, 5(1), 123-127. https://doi.org/10.1099/00222615-5-1-123

36. Giraudo, A. T., Cheung, A. L., & Nagel, R. (1997). The SAE locus of staphylococcus aureus controls exoprotein synthesis at the transcriptional level. Archives of Microbiology, 168(1), 53-58. https://doi.org/10.1007/s002030050469

37. Novick, R. P., & Jiang, D. (2003). The staphylococcal saeRS system coordinates environmental signals with agr quorum sensing. Microbiology, 149(10), 2709-2717. https://doi.org/10.1099/mic.0.26575-0

38. Montgomery, C. P., Boyle-Vavra, S., Adem, P. V., Lee, J. C., Husain, A. N., Clasen, J., & Daum, R. S. (2008). Comparison of Virulence in Community-Associated Methicillin-Resistant Staphylococcus aureus Pulsotypes USA300 and USA400 in a Rat Model of Pneumonia. The Journal of Infectious Diseases, 198(4), 561–570. https://doi.org/10.1086/590157

39. DeLeo, F. R., Kennedy, A. D., Chen, L., Wardenburg, J. B., Kobayashi, S. D., Mathema, B., Braughton, K. R., Whitney, A. R., Villaruz, A. E., Martens, C. A., Porcella, S. F., McGavin, M. J., Otto, M., Musser, J. M., & Kreiswirth, B. N. (2011). Molecular differentiation of historic phage-type 80/81 and contemporary epidemic Staphylococcus aureus. Proceedings of the National Academy of Sciences, 108(44), 18091–18096. https://doi.org/10.1073/pnas.1111084108

40. Montgomery, C. P., Boyle-Vavra, S., & Daum, R. S. (2010). Importance of the Global Regulators Agr and SaeRS in the Pathogenesis of CA-MRSA USA300 Infection. PLoS ONE, 5(12), e15177. https://doi.org/10.1371/journal.pone.0015177

41. Powers, M. E., Kim, H. K., Wang, Y., & Bubeck Wardenburg, J. (2012). ADAM10 Mediates Vascular Injury Induced by Staphylococcus aureus α-Hemolysin. The Journal of Infectious Diseases, 206(3), 352–356. https://doi.org/10.1093/infdis/jis192

42. Inoshima, N., Wang, Y., & Bubeck Wardenburg, J. (2012). Genetic Requirement for ADAM10 in Severe Staphylococcus aureus Skin Infection. Journal of Investigative Dermatology, 132(5), 1513–1516. https://doi.org/10.1038/jid.2011.462

43. O'Callaghan, R. J., Callegan, M. C., Moreau, J. M., Green, L. C., Foster, T. J., Hartford, O. M., Engel, L. S., & Hill, J. M. (1997). Specific roles of Alpha-toxin and

beta-toxin during staphylococcus aureus corneal infection. Infection and Immunity, 65(5), 1571-1578. https://doi.org/10.1128/iai.65.5.1571-1578.1997

44. Hildebrand, A., Pohl, M., & Bhakdi, S. (1991). Staphylococcus aureus Alpha-toxin. Dual mechanism of binding to target cells. Journal of Biological Chemistry, 266(26), 17195-17200. https://doi.org/10.1016/s0021-9258(19)47358-4

45. Wilke, G. A., & Wardenburg, J. B. (2010). Role of a disintegrin and metalloprotease 10 in Staphylococcus aureus -hemolysin-mediated cellular injury. Proceedings of the National Academy of Sciences, 107(30), 13473–13478. https://doi.org/10.1073/pnas.1001815107

46. Valeva, A., Hellmann, N., Walev, I., Strand, D., Plate, M., Boukhallouk, F., Brack, A., Hanada, K., Decker, H., & Bhakdi, S. (2006). Evidence That Clustered Phosphocholine Head Groups Serve as Sites for Binding and Assembly of an Oligomeric Protein Pore. Journal of Biological Chemistry, 281(36), 26014–26021. https://doi.org/10.1074/jbc.M601960200

47. Watanabe, M., Tomita, T., & Yasuda, T. (1987). Membrane-damaging action of staphylococcal Alpha-toxin on phospholipid-cholesterol liposomes. Biochimica et Biophysica Acta (BBA) - Biomembranes, 898(3), 257-265. https://doi.org/10.1016/0005-2736(87)90065-4

48. Ferreras, M., Höper, F., Dalla Serra, M., Colin, D. A., Prévost, G., & Menestrina, G. (1998). The interaction of staphylococcus aureus Bi-component γ-hemolysins and leucocidins with cells and lipid membranes. Biochimica et Biophysica Acta (BBA) - Biomembranes, 1414(1-2), 108-126. https://doi.org/10.1016/s0005-2736(98)00160-6

49. Cassidy, P. S., & Harshman, S. (1973). The Binding of Staphylococcal 125I-α-Toxin (B) to Erythrocytes. Journal of Biological Chemistry, 248(15), 5545–5546. https://doi.org/10.1016/S0021-9258(19)43637-5

50. Hartmann, D. (2002). The disintegrin/metalloprotease ADAM 10 is essential for notch signalling but not for Alpha-secretase activity in fibroblasts. Human Molecular Genetics, 11(21), 2615-2624. https://doi.org/10.1093/hmg/11.21.2615

51. Wetzel, S., Seipold, L., & Saftig, P. (2017). The metalloproteinase ADAM10: A useful therapeutic target? Biochimica et Biophysica Acta (BBA) - Molecular Cell Research, 1864(11), 2071–2081. https://doi.org/10.1016/j.bbamcr.2017.06.005

52. Inoshima, I., Inoshima, N., Wilke, G. A., Powers, M. E., Frank, K. M., Wang, Y., & Wardenburg, J. B. (2011). A Staphylococcus aureus pore-forming toxin subverts the activity of ADAM10 to cause lethal infection in mice. Nature Medicine, 17(10), 1310–1314. https://doi.org/10.1038/nm.2451

53. Becker, R. E. N., Berube, B. J., Sampedro, G. R., DeDent, A. C., & Bubeck Wardenburg, J. (2014). Tissue-Specific Patterning of Host Innate Immune Responses by Staphylococcus aureus α-Toxin. Journal of Innate Immunity, 6(5), 619–631. https://doi.org/10.1159/000360006

54. Powers, M. E., Becker, R. E. N., Sailer, A., Turner, J. R., & Bubeck Wardenburg, J. (2015). Synergistic Action of Staphylococcus aureus α-Toxin on Platelets and Myeloid Lineage Cells Contributes to Lethal Sepsis. Cell Host & Microbe, 17(6), 775–787. https://doi.org/10.1016/j.chom.2015.05.011

55. Valeva, A., Pongs, J., Bhakdi, S., & Palmer, M. (1997). Staphylococcal α-toxin: The role of the N-Terminus in formation of the heptameric pore — a fluorescence study1This work contains parts of the M.D. thesis of Judith Pongs.1. Biochimica et Biophysica Acta (BBA) - Biomembranes, 1325(2), 281-286. https://doi.org/10.1016/s0005-2736(96)00266-0

56. Valeva, A., Palmer, M., & Bhakdi, S. (1997). Staphylococcal α-toxin: formation of the Heptameric pore is partially cooperative and proceeds through multiple intermediate stages. Biochemistry, 36(43), 13298-13304. https://doi.org/10.1021/bi971075r

57. Walker, B., & Bayley, H. (1995). Key Residues for Membrane Binding, Oligomerization, and Pore Forming Activity of Staphylococcal α-Hemolysin Identified by Cysteine Scanning Mutagenesis and Targeted Chemical Modification. Journal of Biological Chemistry, 270(39), 23065–23071. https://doi.org/10.1074/jbc.270.39.23065

58. Sugawara, T., Yamashita, D., Kato, K., Peng, Z., Ueda, J., Kaneko, J., Kamio, Y., Tanaka, Y., & Yao, M. (2015). Structural basis for pore-forming mechanism of staphylococcal α-hemolysin. Toxicon, 108, 226–231. https://doi.org/10.1016/j.toxicon.2015.09.033

59. White, J. M. (2003). ADAMs: Modulators of cell–cell and cell–matrix interactions. Current Opinion in Cell Biology, 15(5), 598–606. https://doi.org/10.1016/j.ceb.2003.08.001

60. Reiss, K., Ludwig, A., & Saftig, P. (2006). Breaking up the tie: Disintegrin-like metalloproteinases as regulators of cell migration in inflammation and invasion. Pharmacology & Therapeutics, 111(3), 985–1006. https://doi.org/10.1016/j.pharmthera.2006.02.009

61. Seegar, T. C. M., Killingsworth, L. B., Saha, N., Meyer, P. A., Patra, D., Zimmerman, B., Janes, P. W., Rubinstein, E., Nikolov, D. B., Skiniotis, G., Kruse, A. C., & Blacklow, S. C. (2017). Structural Basis for Regulated Proteolysis by the α-Secretase ADAM10. Cell, 171(7), 1638-1648.e7. https://doi.org/10.1016/j.cell.2017.11.014

62. Seals, D. F. (2003). The ADAMs family of metalloproteases: Multidomain proteins with multiple functions. Genes & Development, 17(1), 7–30. https://doi.org/10.1101/gad.1039703

63. Stöcker, W., Grams, F., Reinemer, P., Bode, W., Baumann, U., Gomis-Rüth, F.-X., & Mckay, D. B. (2008). The metzincins—Topological and sequential relations between the astacins, adamalysins, serralysins, and matrixins (collagenases) define a super family of zinc-peptidases. Protein Science, 4(5), 823–840. https://doi.org/10.1002/pro.5560040502

64. Wozniak, J., Floege, J., Ostendorf, T., & Ludwig, A. (2021). Key metalloproteinase-mediated pathways in the kidney. Nature Reviews Nephrology, 17(8), 513-527. https://doi.org/10.1038/s41581-021-00415-5

65. Reiss, K., & Saftig, P. (2009). The "A Disintegrin and Metalloprotease" (ADAM) family of sheddases: Physiological and cellular functions. Seminars in Cell & Developmental Biology, 20(2), 126-137. https://doi.org/10.1016/j.semcdb.2008.11.002

66. Janes, P. W., Saha, N., Barton, W. A., Kolev, M. V., Wimmer-Kleikamp, S. H., Nievergall, E., Blobel, C. P., Himanen, J., Lackmann, M., & Nikolov, D. B. (2005). Adam meets Eph: An ADAM substrate recognition module acts as a molecular switch for Ephrin cleavage in trans. Cell, 123(2), 291-304. https://doi.org/10.1016/j.cell.2005.08.014

67. Milla, M. E., Leesnitzer, M. A., Moss, M. L., Clay, W. C., Carter, H. L., Miller, A. B., Su, J., Lambert, M. H., Willard, D. H., Sheeley, D. M., Kost, T. A., Burkhart, W., Moyer, M., Blackburn, R. K., Pahel, G. L., Mitchell, J. L., Hoffman, C. R., & Becherer, J. D. (1999). Specific sequence elements are required for the expression of functional tumor necrosis factor-α-converting enzyme (TACE). Journal of Biological Chemistry, 274(43), 30563-30570. https://doi.org/10.1074/jbc.274.43.30563

68. Clegg, J., Soldaini, E., McLoughlin, R. M., Rittenhouse, S., Bagnoli, F., & Phogat, S. (2021). Staphylococcus aureus vaccine research and development: The past, present and future, including novel therapeutic strategies. Frontiers in Immunology, 12. https://doi.org/10.3389/fimmu.2021.705360

69. Fowler, V. G., & Proctor, R. A. (2014). Where does a Staphylococcus aureus vaccine stand? Clinical Microbiology and Infection, 20, 66–75. https://doi.org/10.1111/1469-0691.12570

70. Proctor, R. A. (2019). Immunity to staphylococcus aureus: Implications for vaccine development. Gram-Positive Pathogens, 766-775. https://doi.org/10.1128/9781683670131.ch48

71. Lee, B., Olaniyi, R., Kwiecinski, J. M., & Wardenburg, J. B. (2020). Staphylococcus aureus toxin suppresses antigen-specific T cell responses. Journal of Clinical Investigation, 130(3), 1122-1127. https://doi.org/10.1172/jci130728

72. Singh, R. A. K., Rodgers, J. R., & Barry, M. A. (2002). The Role of T Cell Antagonism and Original Antigenic Sin in Genetic Immunization. The Journal of Immunology, 169(12), 6779–6786. https://doi.org/10.4049/jimmunol.169.12.6779

73. Davenport, F. M., & Hennessy, A. V. (1957). Predetermination by infection and by vaccination of antibody response to influenza virus vaccines. Journal of Experimental Medicine, 106(6), 835-850. https://doi.org/10.1084/jem.106.6.835

74. Kim, J. H., Skountzou, I., Compans, R., & Jacob, J. (2009). Original antigenic sin responses to influenza viruses. The Journal of Immunology, 183(5), 3294-3301. https://doi.org/10.4049/jimmunol.0900398

75. Midgley, C. M., Bajwa-Joseph, M., Vasanawathana, S., Limpitikul, W., Wills, B., Flanagan, A., Waiyaiya, E., Tran, H. B., Cowper, A. E., Chotiyarnwon, P., Grimes, J. M., Yoksan, S., Malasit, P., Simmons, C. P., Mongkolsapaya, J., & Screaton, G. R. (2010). An in-depth analysis of original antigenic sin in dengue virus infection. Journal of Virology, 85(1), 410-421. https://doi.org/10.1128/jvi.01826-10

76. Focosi, D., Genoni, A., Lucenteforte, E., Tillati, S., Tamborini, A., Spezia, P. G., Azzi, L., Baj, A., & Maggi, F. (2021). Previous humoral immunity to the endemic seasonal Alphacoronaviruses NL63 and 229E is associated with worse clinical outcome in COVID-19 and suggests original antigenic sin. Life, 11(4), 298. https://doi.org/10.3390/life11040298

77. Ragle, B. E., & Bubeck Wardenburg, J. (2009). Anti-Alpha-Hemolysin monoclonal antibodies mediate protection against staphylococcus aureus pneumonia. Infection and Immunity, 77(7), 2712-2718. https://doi.org/10.1128/iai.00115-09

78. Wardenburg, J. B., & Schneewind, O. (2008). Vaccine protection against staphylococcus aureus pneumonia. Journal of Experimental Medicine, 205(2), 287-294. https://doi.org/10.1084/jem.20072208

79. Kennedy, A., Wardenburg, J., Gardner, D., Long, D., Whitney, A., Braughton, K., Schneewind, O., & DeLeo, F. (2010). Targeting of Alpha-hemolysin by active or passive immunization decreases severity of USA300 skin infection in a mouse model. The Journal of Infectious Diseases, 202(7), 1050-1058. https://doi.org/10.1086/656043

80. Tkaczyk, C., Hua, L., Varkey, R., Shi, Y., Dettinger, L., Woods, R., Barnes, A., MacGill, R. S., Wilson, S., Chowdhury, P., Stover, C. K., & Sellman, B. R. (2012). Identification of Anti-Alpha toxin monoclonal antibodies that reduce the severity of staphylococcus aureus Dermonecrosis and exhibit a correlation between affinity and

potency. Clinical and Vaccine Immunology, 19(3), 377-385. https://doi.org/10.1128/cvi.05589-11

81. Hua, L., Cohen, T. S., Shi, Y., Datta, V., Hilliard, J. J., Tkaczyk, C., Suzich, J., Stover, C. K., & Sellman, B. R. (2015). MEDI4893* promotes survival and extends the antibiotic treatment window in a staphylococcus aureus Immunocompromised pneumonia model. Antimicrobial Agents and Chemotherapy, 59(8), 4526-4532. https://doi.org/10.1128/aac.00510-15

82. Tkaczyk, C., Hamilton, M. M., Sadowska, A., Shi, Y., Chang, C., Chowdhury, P., Buonapane, R., Xiao, X., Warrener, P., Mediavilla, J., Kreiswirth, B., Suzich, J., Stover, C. K., & Sellman, B. R. (2016). Targeting Alpha toxin and ClfA with a Multimechanistic monoclonal-antibody-Based approach for prophylaxis of serious staphylococcus aureus disease. mBio, 7(3). https://doi.org/10.1128/mbio.00528-16

83. Lo, M., Aulabaugh, A., Jin, G., Cowling, R., Bard, J., Malamas, M., & Ellestad, G. (2004). Evaluation of fluorescence-based thermal shift assays for hit identification in drug discovery. Analytical Biochemistry, 332(1), 153-159. https://doi.org/10.1016/j.ab.2004.04.031

84. Huynh, K., & Partch, C. L. (2015). Analysis of protein stability and ligand interactions by thermal shift assay. Current Protocols in Protein Science, 79(1). https://doi.org/10.1002/0471140864.ps2809s79

85. Garçon, N., & Di Pasquale, A. (2016). From discovery to licensure, the adjuvant system story. Human Vaccines & Immunotherapeutics, 13(1), 19-33. https://doi.org/10.1080/21645515.2016.1225635

86. Schmidt, G., Papatheodorou, P., & Aktories, K. (2015). Novel receptors for bacterial protein toxins. Current Opinion in Microbiology, 23, 55-61. https://doi.org/10.1016/j.mib.2014.11.003

87. Murata, K., & Wolf, M. (2018). Cryo-electron microscopy for structural analysis of dynamic biological macromolecules. Biochimica et Biophysica Acta (BBA) - General Subjects, 1862(2), 324-334. https://doi.org/10.1016/j.bbagen.2017.07.020

88. Benjin, X., & Ling, L. (2019). Developments, applications, and prospects of cryo-electron microscopy. Protein Science, 29(4), 872-882. https://doi.org/10.1002/pro.3805